Louis AGARD

MNIS / Nanotech
2026

Institut des NanoSciences de Paris
4 place Jussieu, 75005 Paris

Surface lattice resonance in an array of gold nanoparticles

from 16/02/26 to 31/07/26

Under the supervision of :

- **Company supervisor : Agnès MAITRE, agnes.maitre@insp.upmc.fr**
- **Phelma Tutor : Liliana PREJBEANU, liliana.buda@cea.fr**

Confidentiality : no

Ecole nationale
supérieure de physique,
électronique, matériaux

Phelma
Bât. Grenoble INP - Minatec
3 Parvis Louis Néel - CS 50257
F-38016 Grenoble Cedex 01

Tél +33 (0)4 56 52 91 00
Fax +33 (0)4 56 52 91 03

http://phelma.grenoble-inp.fr

Contents

1 Introduction 1
2 Plasmonic Resonance 2
2.1 Collective Oscillation of a metal electron cloud - Localized Surface Plasmon 2
2.2 Localized Surface Plasmon Resonance (LSPR) 2
2.3 Surface Lattice Resonance (SLR) 3
2.4 SLR theory - Coupled Dipole Approximation 4
2.5 SLR theory - Rayleigh anomalies 6
2.6 Link between Rayleigh anomalies and SLR 7
3 Nanofabrication of samples 8
3.1 Context 8
3.2 Nanoparticle Array Process Flow 9
3.3 SEM observation of the array 12
4 Detection of plasmonic resonance 14
4.1 Experimental setup 14
4.2 Data treatment 15
4.3 Interpretation 16
4.4 Symmetric/Asymmetric environments 17
4.5 Collective resonance damping in asymmetric environments . . 18
5 Plasmonic resonance with ITO in asymmetric environment 19
5.1 ITO overview 19
5.2 Clean room implementation 20
5.3 Collective resonances with ITO 20
5.4 Comparison with simulations 21
5.5 Conclusion and perspectives 25
6 Creation of cavities 26
6.1 Cavity theory - Purcell effect 26
6.2 Fabrication of the cavities 27
6.3 Characterization 27
6.4 Cavity extinction spectra : sample with ITO substrate 29
6.5 Cavity extinction spectra : sample without ITO substrate . . 30
7 Introducing nanoemitters on top of the lattice 31
7.1 Quantum Dot introduction 31
7.2 Presentation of the QDs used 31
7.3 Deposition of nanoemitters on a sample 32
7.4 Characterization of the Quantum Dots in the lattice 33

8 Introducing nanoemitters inside the cavities 36
8.1 Preliminary study - Optimal PMMA thickness for QDs 36
8.2 Perspectives 38
9 Conclusion 39

A Gantt Diagram **42**

B Résumés **43**

1 Introduction

The Institut des NanoSciences de Paris (INSP) is a joint research unit of Sorbonne Université and the CNRS, specialized in condensed matter physics and nanoscience. Its research focuses on understanding and controlling physical phenomena that emerge at the nanoscale, particularly at interfaces and within systems where characteristic lengths are smaller than the studied objects. The institute combines expertise in nanofabrication, with a dedicated clean room inside the institute, along with experimental and theoretical expertise.

Within INSP, the "Acoustics and Optics for Nanosciences and Quantum" (ACONIQ) team investigates light and sound interactions at the nanoscale. Their work includes the generation and detection of acoustic phonons, ultrafast optical measurements, and the manipulation of light-matter interactions in nanostructures. This group's research is at the intersection of nanophotonics and quantum science, contributing to both fundamental understanding and potential technological innovations.

Within INSP and ACONIQ, I was a part of the NANOOQ team, which consists of 3 PhD students, 1 intern, 1 engineer, and 1 professor.

In this team, I had the opportunity to work on Plasmonic Surface Lattice Resonance (SLR), in the context of light-matter interaction in nanostructures. It has been proven by the NANOOQ team a few years ago that coupling a Quantum Dot (QD) to a single plasmonic patch antenna enhanced emission [2]. My work followed this framework by implementing a collective patch antenna powered by SLR, to have both enhanced emission of the QDs and a collective emission. My first task was to fabricate and characterize nanoparticle arrays that would exhibit a form of plasmonic collective resonance. Afterwards, my goal was to create cavities on top of those arrays, with and without QDs, look at its coupling conditions and characterize its optical properties.

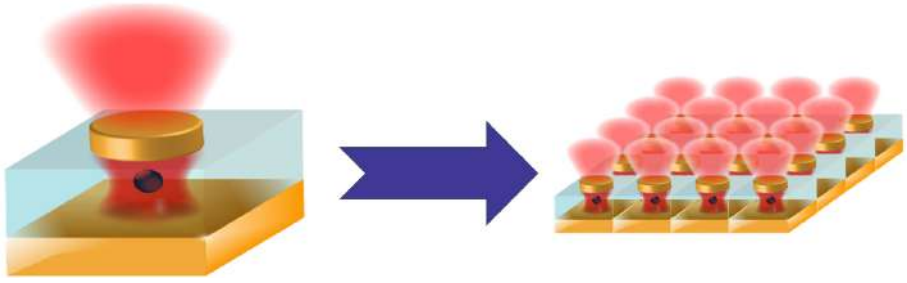


Figure 1: Left : Schematic of an enhanced emission of a nanoemitter when coupled to a single patch antenna. Right : Schematic of an enhanced and coherent emission of nanoemitters when coupled to a lattice of antennas. This structure will be the objective of the internship.

2 Plasmonic Resonance

2.1 Collective Oscillation of a metal electron cloud - Localized Surface Plasmon

Before discussing Plasmonic Resonance, we must first introduce Plasmons, which are collective oscillations of electron density in a metal. To illustrate this phenomenon, let us take a gold sphere of radius a immersed in air. The conduction electrons of the sphere form what is called an "electron cloud". When an incident light of an electric field E_0 impinges onto the sphere, this electron cloud is displaced by the oscillation of the wave electric field.

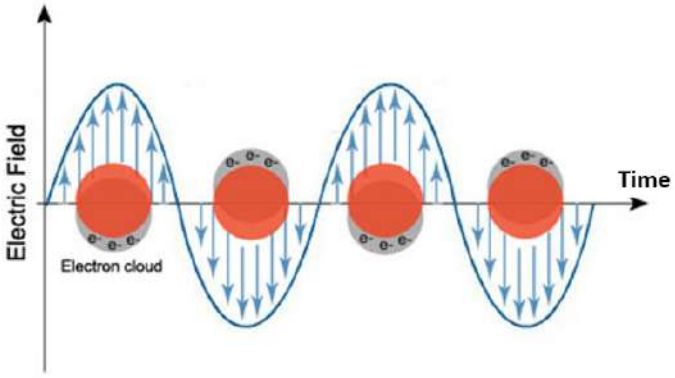


Figure 2: Schematic representing the oscillation of the electron cloud of a metal sphere, depending on time and the value of the incident electric field.

The incident light causes the electron cloud to oscillate. This is called Localized Surface Plasmon. The oscillating electrons form an oscillating dipole of polarization P :

$$P = \alpha \cdot E_0 \tag{1}$$

α being the polarizability of the sphere.

2.2 Localized Surface Plasmon Resonance (LSPR)

For a sphere of radius a immersed in air, its polarizability is expressed as such :

$$\alpha = 4\pi a^3 \cdot \frac{\epsilon(\omega) - 1}{\epsilon(\omega) + 2} \tag{2}$$

with ϵ the permittivity of the material, which depends on the wavelength.

When $\Re(\epsilon) = -2$, which is a viable value for a metal, the polarizability and thus the induced polarization admit a maximum resonance.

The created dipole will, at this frequency, absorb more light and let less pass through the object. This will in turn create a resonance in light absorption (and in transmission), as seen in fig. 4, at a certain wavelength. (a). This specific resonance is called **L**ocalized **S**urface **P**lasmon **R**esonance, and will be referenced as **LSPR** from now on.

To quantify the resonance peak, let us introduce the quality factor Q.It is defined as $Q = \frac{\lambda_{max}}{\Delta\lambda}$, the ratio of the resonance wavelength λ_{max} to the full-width at half maximum. The higher the quality factor, the thinner and the higher the resonance. What we want is the highest Q possible.

For a standard LSPR peak, Q is generally around 10, which is relatively low. Although this resonance can and has been used for plasmonic applications (see [9] for example), it is possible to have a higher-Q plasmonic resonance.

2.3 Surface Lattice Resonance (SLR)

One way to try to enhance plasmonic resonance is by implementing an array of nanoparticles instead of just a single one. Each of those nanoparticles, under incident light, will act as a dipole. The dipolar fields of the particles will interact with each other, and alter the polarization of the particles around them.

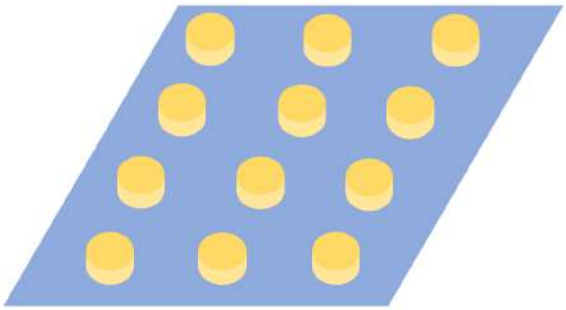


Figure 3: Left : Schematic of 2D array of nanoparticles on a substrate.

This will in turn create a new collective resonance of the array, instead of an isolated resonance of the particle. This resonance has a much higher Q (around 100) than that of a single nanoparticle resonance (LSPR) . This phenomenon is called **S**urface **L**attice **R**esonance (**SLR**).

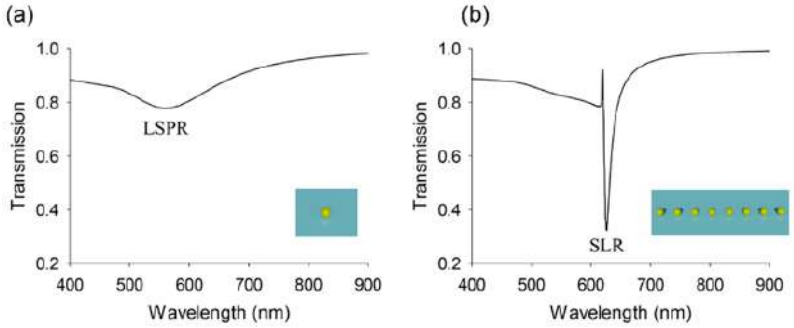


Figure 4: Transmission spectra of a line of gold particle of 80nm radius, exhibiting SLR. The resonance is much thinner and higher in terms of intensity. [8]

Surface Lattice resonance will be the main focus of the internship, the objective being to fabricate and characterize nanoparticle arrays exhibiting SLR. In our case, we will have particles in disk shape rather than spheres, because it is easier to fabricate.

2.4 SLR theory - Coupled Dipole Approximation

To look at the theory behind Surface Lattice Resonance, we need to represent the array of nanoparticles as an array of coupled dipoles.

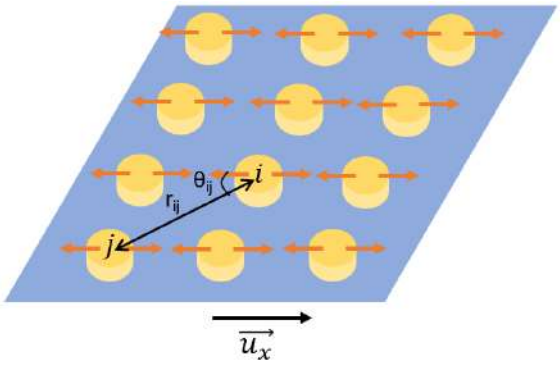


Figure 5: Schematic of the nanoparticles array. the orange arrows represent the direction of the dipole. Nanoparticle i is showcased as well. The nanoparticles are illuminated by an incident plane wave $\vec{E_0}$ of polarization $\vec{u_x}$.

According to Coupled Dipole Approximation (CDA), we can write the induced polarizability of one particle i in the array as the sum of the incident field E_0 and the contribution of all dipole fields of the other particles around it :

$$P_i = \alpha \left(E_0 + \sum_{i \neq j} E_{\text{dipole},j} \right) \tag{3}$$

In the approximation that the array is infinite (viable if there are many particles in the array), we can state that the induced polarization is the same for all the particles : $\forall i, P_i = P$. Because of the interaction of the other dipolar fields, the field associated to each nanoparticle can thus be expressed simply as a function of the induced polarization :

$$\forall j, E_{\text{dipole},j} = S \cdot P \tag{4}$$

With S being a geometrical parameter depending on the array geometry :

$$S = \sum_{j \neq 1} \left[\frac{(1 - ik \cdot r_{ij})(3\cos^2\theta_{ij} - 1)e^{ik \cdot r_{ij}}}{r_{ij}^3} + \frac{k^2 \sin^2\theta_{ij} e^{ik \cdot r_{ij}}}{r_{ij}} \right] \tag{5}$$

with r_{ij} the distance between the particle i and j and θ_{ij} the angle taken from the direction of the dipole i to the particle j (see fig. 5).

From this, you can express the induced polarization of a particle i as an expression of the incident field, by injecting (4) into (3) :

$$P = \frac{1}{\frac{1}{\alpha} - S} E_0 = \alpha' E_0 \tag{6}$$

with α' being the effective polarizability of the particle. The array modifies the effective polarizability of the particle, and also changes its resonance condition. Here, α' reaches a maximum when $\Re(\frac{1}{\alpha(\lambda)}) = \Re(S)$.

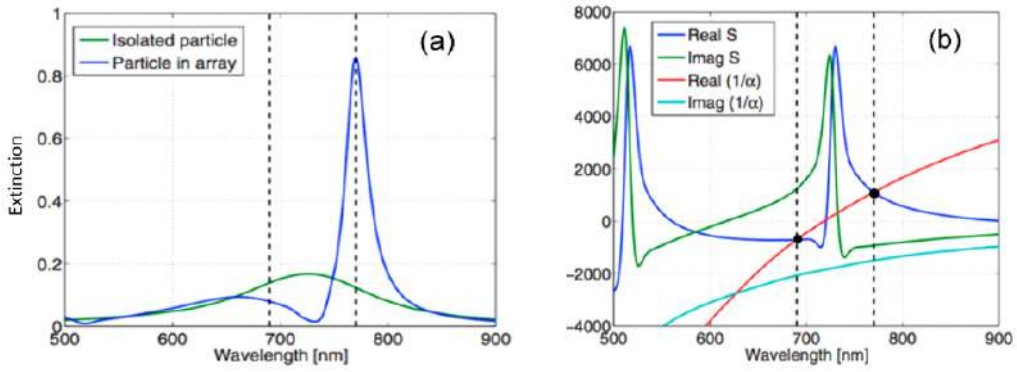


Figure 6: (a) Extinction cross section for an isolated particle and for a square array of period 480nm. The nanoparticles are silver nanodisks of diameter 120nm and height 30nm. (b) Calculated dipole sum and polarizability (both real and complex parts) depending on the frequency. The vertical dashed lines correspond to the wavelengths where $\Re(\frac{1}{\alpha(\lambda)}) = \Re(S)$.[8]

There are several things to note about fig. 6.

First, we see here ((a)) how implementing an array of nanoparticles yields a stronger and thinner resonance than with an isolated particle. The factor of quality for a SLR is generally around 100.

Furthermore, the SLR occurs at around 770nm, which corresponds exactly to the wavelength where $\Re(\frac{1}{\alpha(\lambda)}) = \Re(S)$ (Fig fig. 6 (b)), confirming the theory mentioned above.

2.5 SLR theory - Rayleigh anomalies

Another way to look at surface lattice resonance is by stating that the nanoparticle array acts as a grating that diffracts incident light. This means that when light impinges onto the lattice, the former is diffracted into several orders, following the grating relation :

$$d(\sin\theta_i + n_1 \sin\theta_p) = p\lambda \tag{7}$$

with d the lattice period, p the order of diffraction, n_1 the refractive index of the substrate, λ the wavelength and $\theta_{i,p}$ the angle of the incident light and the p^{th} diffraction order, respectively.

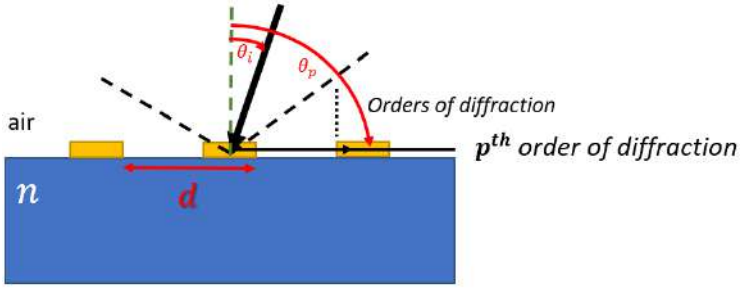


Figure 7: Schematic of a 1D nanoparticle lattice. The incident light is represented by a black arrow, and its diffraction orders are shown in dashed black lines. The p^{th} order of diffraction is showed as in-plane.

If we take a normal incidence ($\theta_i = 0°$) and the p^{th} order of diffraction propagating perpendicularly to the incident light ($\theta_p = 90°$, as showed in fig. 7), the grating relation becomes, for a 1D grating :

$$\lambda_R = \frac{d}{p} \cdot n_1 \tag{8}$$

λ_R is the Rayleigh wavelength of the p^{th} order. This means that at this wavelength, the p^{th} order of diffraction is in plane, and interacts with the other nanoparticles on its path.

For a 2D grating and for normal incidence illumination, which is the case of our sample, the expression has to take into account diffraction along the 2 dimensions :

$$\lambda_R^{(p,q)} = \frac{n_1}{\sqrt{\left(\frac{p}{d_x}\right)^2 + \left(\frac{q}{d_y}\right)^2}} \tag{9}$$

with d_x, d_y the periods along x and y, and p, q the orders of diffraction along these 2 directions respectively.

2.6 Link between Rayleigh anomalies and SLR

Figure fig. 8 shows the correlation between the surface lattice resonance and the Rayleigh anomalies.

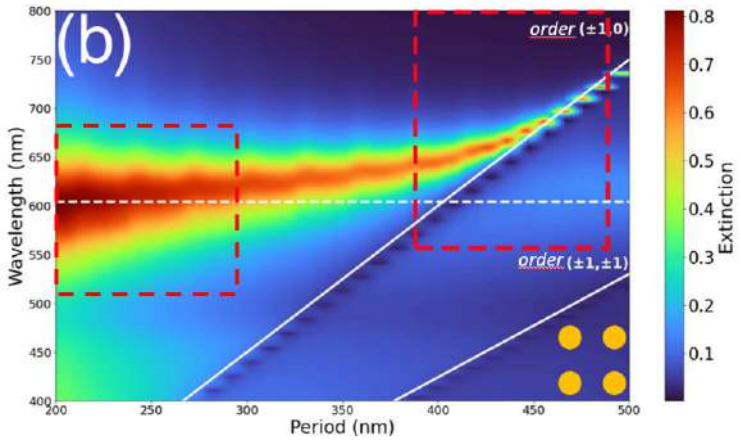


Figure 8: Simulated normal incidence extinction heatmap for gold square arrays of nanodisks, of 80nm diameters and 50nm height as a function of the period of the array. Solid white lines show the theoretical position of the RA (for $n_1 = 1.518$), and horizontal dashed lines correspond to the spectral position of the simulated single-particle LSPR [4].

From this graph, we can pinpoint two important zones that are circled in red :

Low Period : In this zone, there is a large high-extinction zone centered around the LSPR wavelength. This large resonance resembles a single-particle resonance (LSPR). The nanoparticles, at low period and for this bandwidth (400-800nm), do not exhibit collective behavior.

Large Period (>400nm) : When increasing the period, we see that the high-extinction zone becomes thinner and thinner in wavelength, which corresponds to a collective resonance of the nanoparticles (SLR).

Furthermore, we see that this thin extinction zone follows the first-order Rayleigh wavelength equation ($\lambda_R = d \cdot n_1$) when changing the period.

This ultimately shows that the SLR is linked to the Rayleigh Anomaly: The nanoparticles are coupled to each other by the in-plane diffracted light.

3 Nanofabrication of samples

3.1 Context

My first goal in this internship was to create samples that exhibit Plasmonic Surface Lattice Resonance. The blueprint is a 2D matrix of gold nanoparticles on top of a glass substrate. Whilst the radiuses of the particles would remain each time at around 140nm, the periods of the lattice would change along both directions. This would allow to look at the influence of this parameter on the resonance peak, whilst the LSPR peak remains constant, at around 700nm.

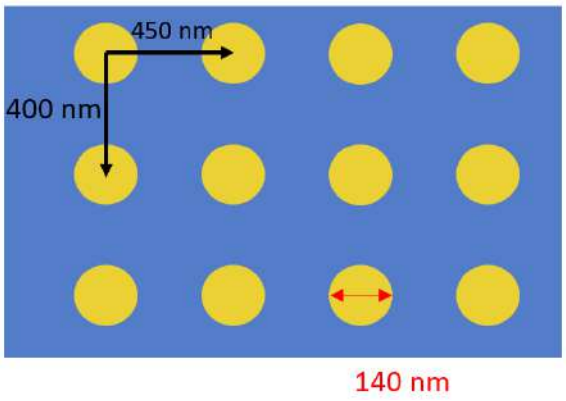


Figure 9: Schematic representing an expected layout for a plasmonic lattice, including the expected periods and radiuses.

Theoretically, this structure would allow for SLR peaks, at the wavelength corresponding to the first order of Rayleigh anomaly (as shown in theory).

To fabricate these samples, I did it entirely in the INSP clean-room, using techniques such as electron-beam lithography, Physical Vapor Deposition (PVD) and Sputtering.

To ensure the quality of the fabrication once it is over, I observed them through a Scanning Electron Microscope (SEM).

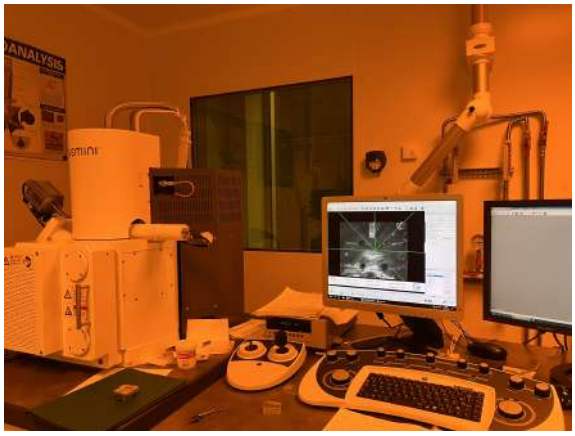


Figure 10: Picture of the SEM/E-beam lithography machine inside the INSP clean-room

3.2 Nanoparticle Array Process Flow

To do the fabrication of our sample, a strict protocol has to be followed. Parameters of this protocol were all optimized (partially by me) in order to create structures of this size.

Overview

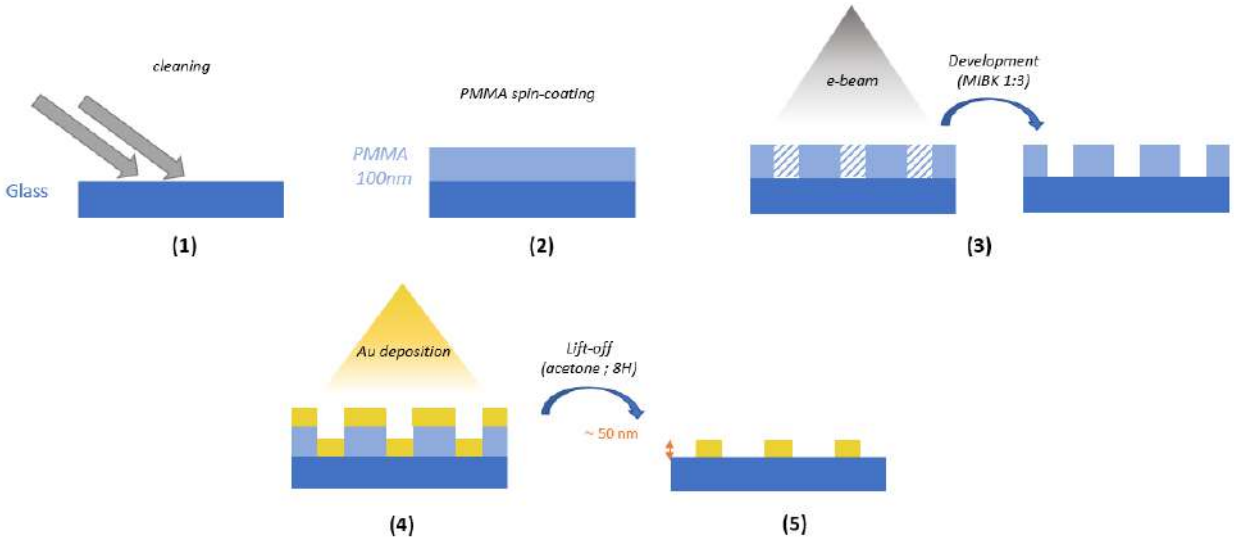


Figure 11: Nanofabrication Process steps of the samples

This process flow, shown in fig. 11, shows a 5-step recipe that will be detailed below.

Substrate choice (1)

The substrate chosen is a borosilicate cover-slip of dimensions $20mm \times 20mm$. It is cleaned with acetone in an ultrasound bath (37Hz) for 5 min. Afterwards, it is cleaned with isopropanol, and in a high power plasma cleaner (60%) for 5 min. The

plasma cleaner remove all residue present on the surface. A gas cloud (here oxygen) will be excited and ionized, forming a plasma. This plasma interacts with the surface of the sample and will remove impurities (mostly organic ones) by chemically reacting with them.

The cleanliness of the sample has to be ensured before going into the next step. A dirty substrate will lead to an inhomogeneous sample, a bad adherence of metals after the lithography and unwanted metal shards after the lift-off.

PMMA deposition (2)

Using a spincoater, a 100 nm PMMA solution is deposited on the sample. The parameters of the spincoater are : 10 sec at 1000rpm + 60 sec @ 4000rpm.

This layer of PMMA will act as a resist for the e-beam lithography.

After coating, the sample is baked for 2 minutes on a hot plate at 180°C to remove the solvent and improve uniformity of the layer.

Electron-beam lithography and development (3)

Electron-beam lithography is a practice consisting of focusing an electron beam on a sample to etch patterns on it. When focused onto a resist (for example PMMA), the solubility of the resist will change and it will be dissolved during the development. The main advantage of this technique, compared to standard optical lithography, is that it can draw shapes down to the 10nm scale, whereas standard optical lithography is limited by its diffraction limit (around 200nm at the very best).

Lithography is performed in the cleanroom with a Zeiss Gemini SEM (shown here : fig. 10) coupled with a software that turns the microscope into a lithography machine. Since our samples are not conductive when using a glass substrate, we need to add a 10 nm layer of aluminum on top of the PMMA by PVD, to help evacuate the charges during lithography.

The lattice pattern (*PositionList*) has to be done beforehand on the software, and lithography usually takes between 3 to 4 minutes for a 100×100µm lattice.

Many lithography parameters have to be tweaked and optimized to ensure the best possible fabrication of our lattices. The optimized values are written in table 1 :

Table 1: Main electron-beam lithography exposure parameters.

Parameter	**Value**
Acceleration Voltage (HV)	20 keV
Aperture Size	10 μm
Beam Current	between 25 and 50 pA
Exposure Dose	240 μC/cm^2
Writefield Size	100 μm × 100 μm (Mag ×490)

Writefield : definition and choice The writefield of the lithography is the area (in µm×µm) where the beam can write. In our case, a higher writefield means a bigger lattice, and ultimately higher signal during the detection. However, the quality of the lattice worsens (irregular particles, vacancies,...) when increasing the writefield.

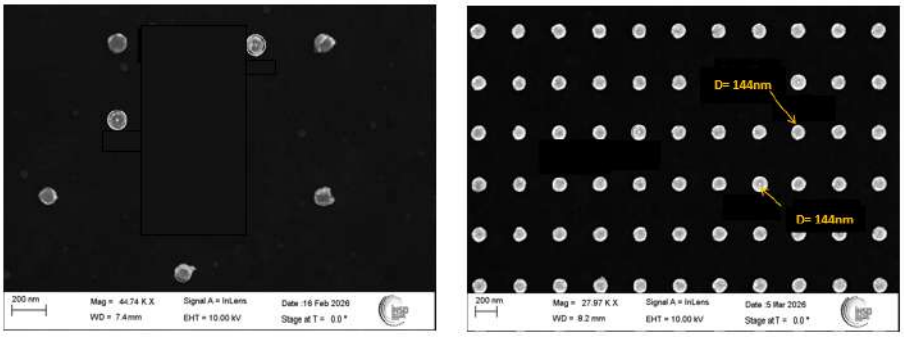


Figure 12: Left : SEM picture of a sample lattice with a writefield of 500×500µm. Particles are irregular in shapes and a lot are missing. Right : SEM picture of a lattice sample with a writefield of 100µm. Here the lattice is much better, both in partice size and in regularity of the particles.

We ultimately chose a smaller writefield for the lithography. In order to have sufficient signal for detection, small 100µm*100µm lattices are drawn right next to each other, in order to have a bigger lattice of high quality. Some gaps are present in between the lattices, as the lithography machine doesn't have an interference plate to have perfect fitting between the 100µm*100µm lattices (see fig. 13). However, it is good enough to exhibit high enough signal during detection, as the gap of 1µm is much smaller than the size of an array.

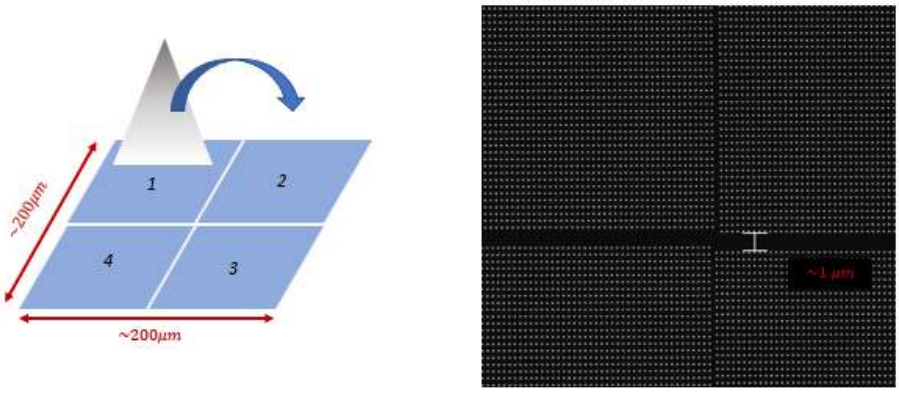


Figure 13: Left : Schematic representing the lithography of a 200×200µm lattice by writing 4 100×100µm lattices next to each other. Right : SEM picture showing the gap between the small lattices. Here the gap is around 1 µm wide.

Once lithography has been performed, the sample is developed with MIBK 1:3 to remove the part of PMMA exposed to the beam. The development lasts 1 min,

and the sample need to be agitated during it. Duration of development has been optimized to avoid either underdevelopment or overdevelopment. In fact, if the development time is too short, the fragmented PMMA chains within the exposed regions are not completely cleared. This leaves residual resist the bottom of the layout, leading to bad quality deposition later on, in terms of adherence and homogeneity of the particles. On the other hand, excessive development time causes the solvent to attack the unexposed or partially exposed sidewalls of the resist. This results, when depositing, in an oversizing of the particles comparing to what was intended in the design.

Gold deposition (4)

To remove all residue inside the developed holes, the sample is put into the plasma cleaner at 15% power and for 3 min. The parameters are lower than in step (1) to maintain the integrity of the structure. Residue inside the holes reduce the quality of the gold deposition, leading to bad quality and/or missing particles after lift-off.

A layer of 40 nm of Gold is then deposited on the sample using Physical Vapor Deposition (PVD). Underneath this layer, a 5nm Titane layer is needed, to ensure adherence of the metal to the surface, since gold on its own does not stick well to glass. This layer is deposited using PVD just like before with gold.

Lift-off (5)

The sample was placed in a beaker filled with acetone for several hours, causing the PMMA layer to dissolve. The gold deposited directly onto the substrate (in the developed part of PMMA) will be unaffected during this process. The fabrication is then finished by spraying acetone with a syringe onto the sample. The high-pressure spray will help remove the dissolved PMMA layer from the sample, leaving only the lattice just like in fig. 11 (5).

The average time to do one sample following this process flow is around 2 full days. During the internship, I did around 20 samples with different parameters and sometimes different substrates.

3.3 SEM observation of the array

Once the lift-off is over, it is necessary to look under the Scanning Electron Microscope (SEM) our lattices to look whether the lithography has been performed successfully or not. The same machine used to perform the lithography is now used for observation. Due to the diffraction limit of the electrons being much smaller than the optical one, SEM allows us to observe the sample in the range of 10nm which enough to observe our nanoparticles with precision.

From those pictures, we can extract the periods of our lattice as well as the size of our nanoparticles. The SEM software provides tools for these measurements.

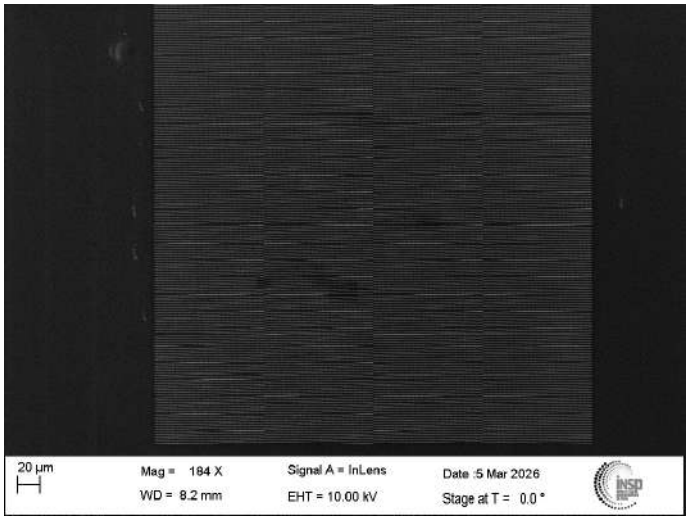


Figure 14: Nanoparticle lattice pictured in the SEM in the sample named GlIe-7. Here, the width of the lattice is of 400µm. You can see the small 100*100µm lattices that form the whole lattice.

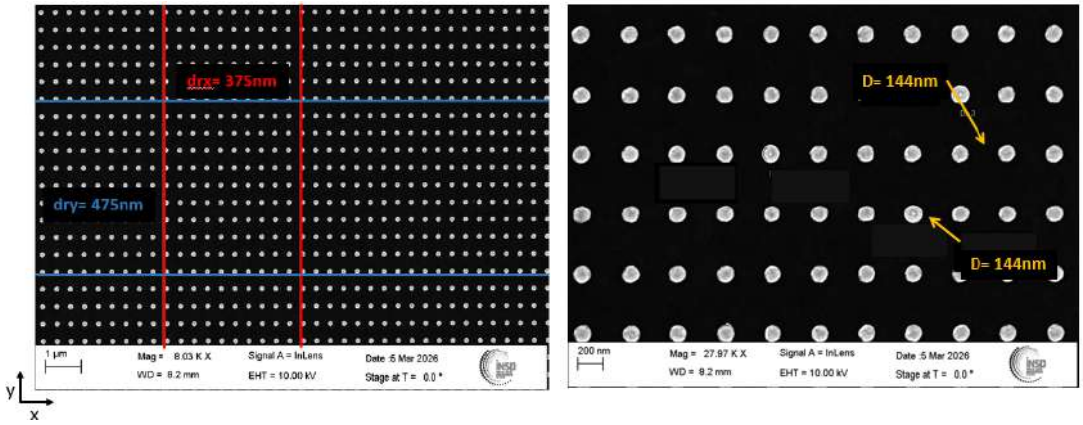


Figure 15: Left: SEM picture of a gold lattice. The red and blue lines correspond to 10 times the period along x (red) and along y (blue). Right: Zoomed picture of the lattice. From this, tools in the SEM allow to extract the diameters of the plots.

Here, the periods are different along the x and y axes. This would allow to detect 2 different signals in one lattice by just changing the polarization of the incident light. We usually obtain nanoparticles of 70nm radius of good quality and high homogeneity. It is possible to fabricate even smaller particles, but here we choose the same radius for all samples, in order to have better comparison between them.

4 Detection of plasmonic resonance

4.1 Experimental setup

Once the sample has been fabricated and observed to confirm its quality, we can try to detect the plasmonic resonances using an optical setup, by measuring its transmission spectra in the visible range.

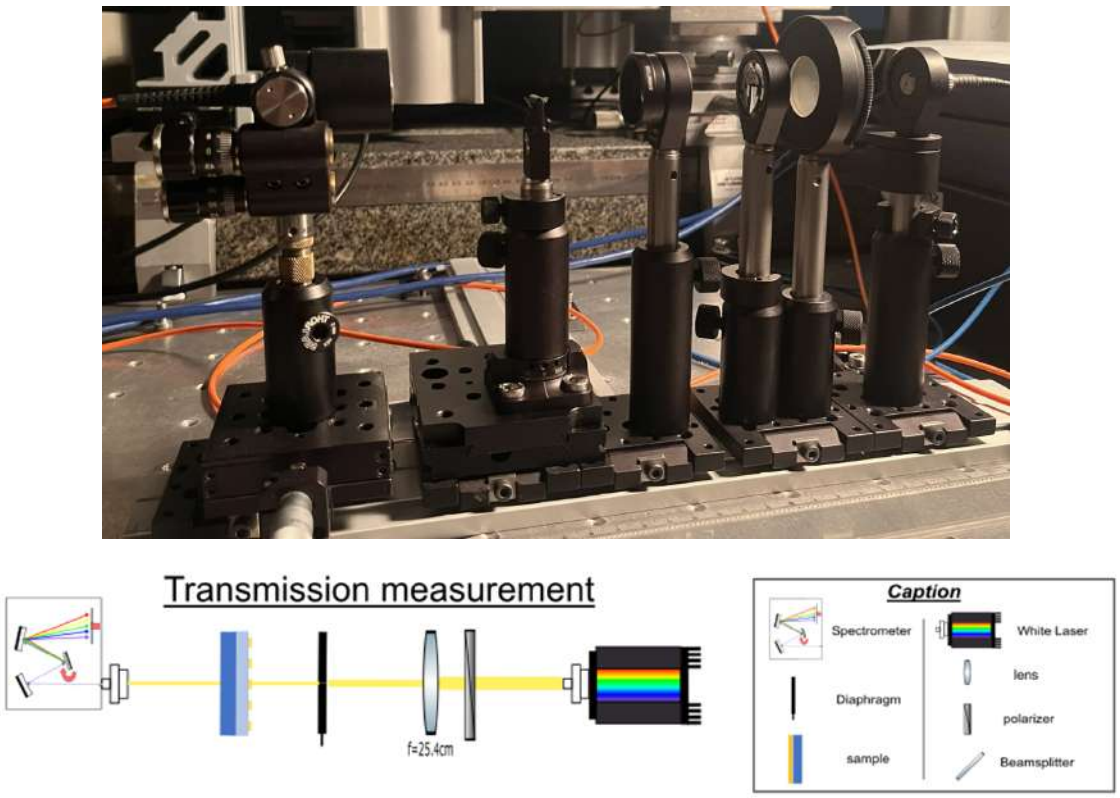


Figure 16: Top : Picture of the experimental setup in the laboratory. Bottom : Schematic of the experimental setup.

This setup shown in fig. 16 has a light source which is a white laser : a laser at 810nm coupled with a photonic fiber, which, with non-linear properties, will give a collimated laser with a spectrum ranging from 450nm to 2µm.

This light passes through a polarizer. Polarizing this light allows us to excite one direction of the lattice at a time. The light is then focused with a lens of focal length $f = 25.4cm$, and passes through a diaphragm. The beam is then impinged onto the sample. Part of the beam is diffracted and/or absorbed by the gold lattice in the sample, while the rest crosses it. The transmitted light is then gathered by a collimator which sends the signal to an optical fiber linked to a spectrometer.

4.2 Data treatment

To have a relevant signal in the spectrometer while not saturating it, the integration time needs to be optimized. For a laser of full power (here 5mW according to the datasheet of the laser), we usually need 300 to 500µs of integration time. The signal is then averaged 10000 times to have a stable output, independent of the laser fluctuations.

To retrieve the transmission spectrum, and afterwards the extinction spectrum, we need to collect 3 different signals :

- A **dark** signal, which is taken with the laser turned off.

- A **reference signal**, which is the white laser passing through the substrate but **not** through the lattice. Choosing this reference allows us to take the reflection/absorption of the glass substrate in consideration.

- The transmitted light after **passing through** the lattice.

By doing the ratio $\frac{I_{sample}-I_{dark}}{I_{ref}-I_{dark}}$, the lattice signal over the reference signal using a Python script, we find the transmission spectra :

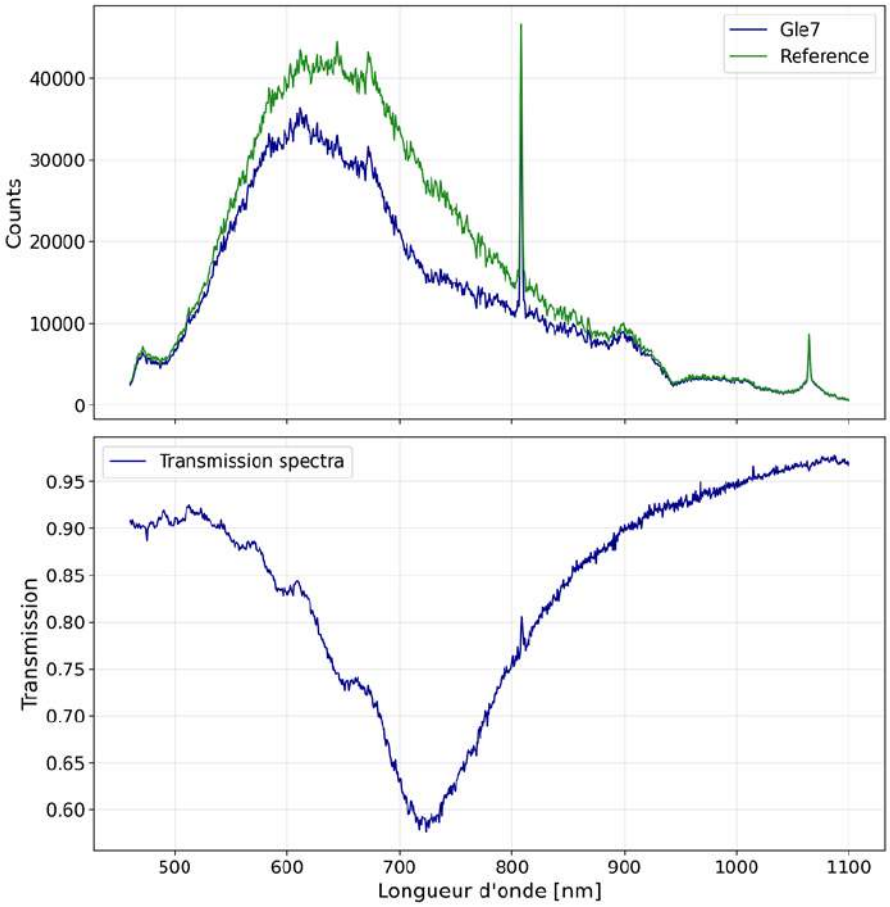


Figure 17: Top : Reference and Lattice signal collected by the spectrometer in the setup. The lattice here has a period of 400nm along both direction. Bottom : Transmission spectra calculated from the 2 signals $(\frac{I_{sample}-I_{dark}}{I_{ref}-I_{dark}})$. The 2 very sharp peaks correspond to the initial pump laser modes, where $\lambda = 810nm, the one which is pumping the white laser$.

From later on, we will start plotting the extinction spectrum rather than the transmission one, as it allows more clear visualization of the peaks.

4.3 Interpretation

On fig. 17, the transmission spectra has a large resonance peak, corresponding to LSPR but not SLR. This means that the resonance is not due to a collective phenomenon of all the particles in the lattice, but rather the incoherent sum of all single particle resonances.

Our goal fabricating nanoparticle arrays is precisely to create samples exhibiting collective resonance. From this result, we decided to change the structure of our sample to allow the observation of SLR. The problem, as shown in literature [7], stems from the fact that the sample considered is asymmetric. This will be detailed in the following lines.

4.4 Symmetric/Asymmetric environments

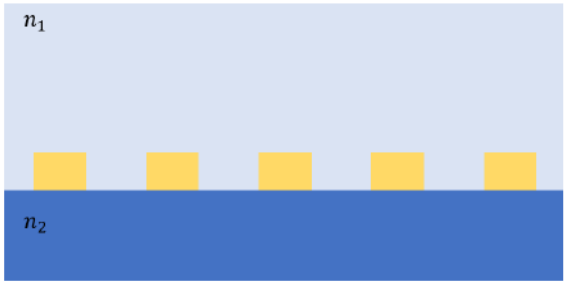


Figure 18: 2D schematic of a standard sample, in an asymmetric environment ($n_1 \neq n_2$).

To understand why we could not manage to have thin high-Q SLR peaks experimentally, let us look at the structure of our sample. The gold lattice here is in an asymmetric environment, which means that the refractive index of the environment ($n_1 = 1$ in air) is different from that of the substrate ($n_2 = 1.5$ for glass) : $n_1 \neq n_2$.

However, Surface Lattice Resonance can be observed mostly in symmetric environments (where $n_1 = n_2$) [7] : This means that the environment of the lattice is a layer which has the same refractive index as the substrate of the sample.

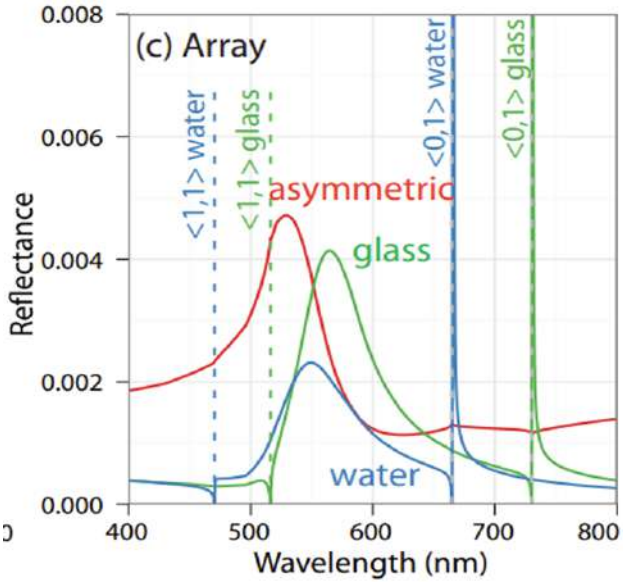


Figure 19: Simulated reflectance spectra for a particle array of period a = 500 nm , also including the asymmetric configuration in which the spheres are in water with their surfaces located at a distance of 1 nm from a glass substrate. Vertical dashed lines indicate the position of the $< 0, 1 >$ and $< 1, 1 >$ Rayleigh anomaly conditions in the different media. All gold nanospheres are taken to have a radius of 35 nm. Taken from [1].

In fig. 19 sharp peaks at the Rayleigh Anomaly condition are present in the water

(blue) and glass (green) symmetric configurations. However, for the asymmetric water/glass configuration, those peaks are nonexistent and only the wide LSPR peak is present.

4.5 Collective resonance damping in asymmetric environments

In the literature, theoretical studies ([1]) have shown why SLR is suppressed in asymmetric environments :

When the incident light impinges into the lattice, it is diffracted in the plane (Rayleigh anomalies), but another interaction happens at the interface between the substrate and the superstrate. There, light is partially reflected and will interfere with the Rayleigh anomalies. By degrading the Rayleigh anomalies, long-term coupling between the nanostructures will also be affected. That will completely suppress collective resonance, leaving only isolated plasmonic absorption (LSPR). This explanation can explain why we cannot see the collective resonance in fig. 17.

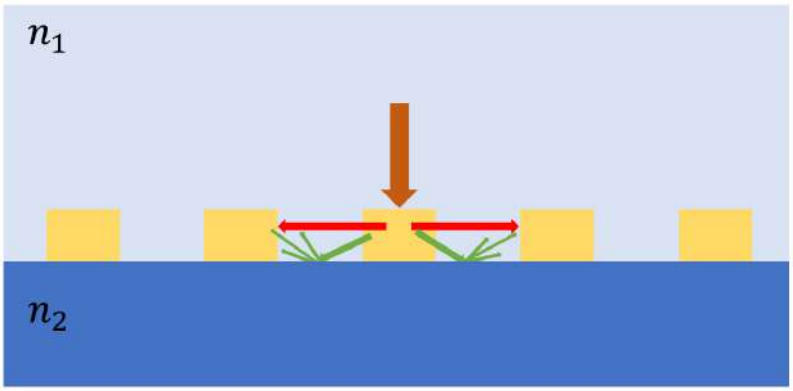


Figure 20: Schematic representing graphically the suppression of long-range coupling in an asymmetric environment. The incident field is represented in orange, the in-plane diffraction is in red and the reflection at the interface substrate/superstrate is in green.

5 Plasmonic resonance with ITO in asymmetric environment

To exhibit collective resonance in an asymmetric environment, we introduced a layer of Indium Tin Oxide (ITO) in our substrate, between the glass substrate and the array (fig. 21). This new layer, as shown in [11], can help retrieve sharp collective resonances, analogous to SLR peaks.

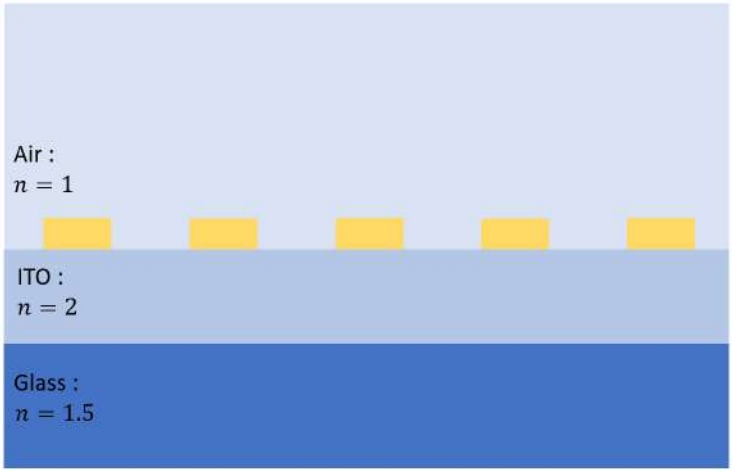


Figure 21: Schematic of the updated sample including the middle ITO layer. Optical indexes n of each layer are written, as well as the thickness of the ITO layer.

5.1 ITO overview

Indium Tin Oxide is a transparent conductive oxide, widely used in photonics and sensing applications. Indeed, this material has very good optical characteristics : It has both a high refractive index n and a low k, making it transparent in the visible range.

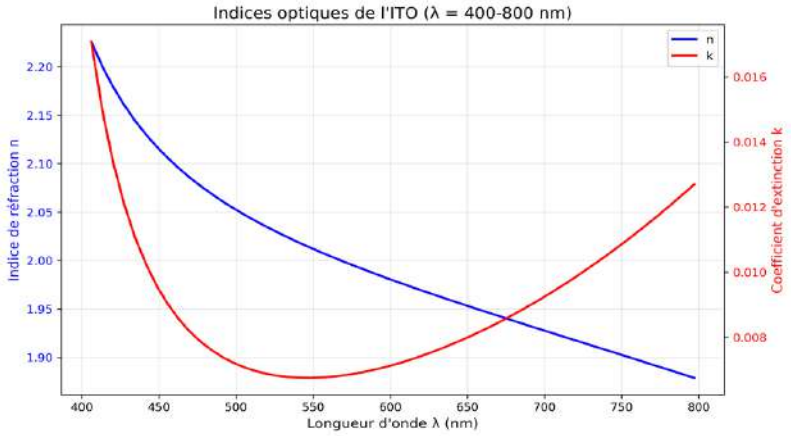


Figure 22: Optical indexes of the ITO sputtered in the INSP cleanroom, found doing ellipsometry.

High n will cause the ITO layer to act as a waveguide, trapping the electric field inside [ref]. This new waveguided mode will couple the nanoparticles dipoles together. Collective resonance in asymmetric environments is thus possible in this configuration, with a slightly different way than with standard SLR. This as been shown before in literature, for example in [3].

5.2 Clean room implementation

Some slight changes to the process flow have to occur in order to implement ITO in our samples.

The ITO layer needs to be deposited using a sputtering machine, with a power of 50W DC, and a deposition time of 1700sec, in order to deposit an ITO layer of 140nm on the substrate.

This value that can be checked using a profilometer, as shown belon in fig. 23.

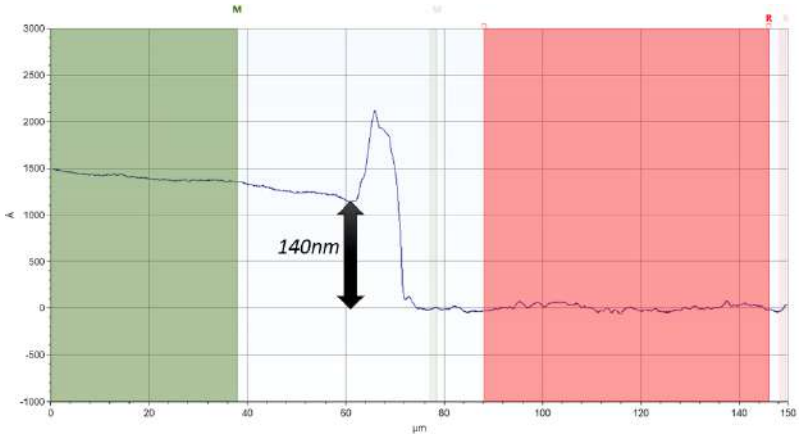


Figure 23: Profilometer curve. The red zone correspond to the glass substrate height, while the green zone correspond to the ITO height. The black arrow exhibit the value of the ITO thickness layer extracted from the profilometer.

Besides this step, the process flow is almost the same for a sample with ITO than for one without it, starting from the cleaning of the substrate. The only difference is that there is no need to add a layer to discharge the sample during the lithography/SEM, since ITO is a conductive material.

5.3 Collective resonances with ITO

These new samples with an ITO substrate were characterized by transmission spectroscopy, in the same way as before. This is possible because our ITO is transparent (see fig. 22).

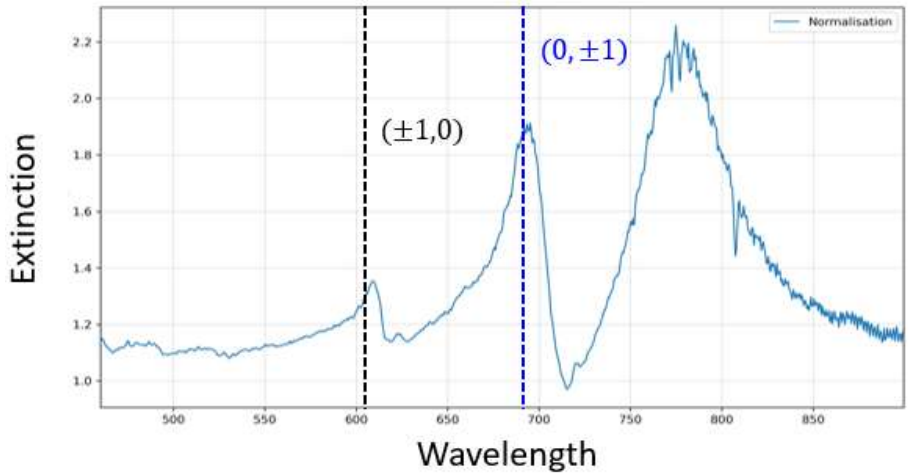


Figure 24: Absorption spectra for a sample with glass/ITO sample. The periods are here of 400nm along x and 450nm along y. Incident light is polarized along y. Black and blue dashed lines represent the 1^{st} order Rayleigh anomaly condition along x (black) and y (blue) (for n_{eff}=1.52).

The extinction spectrum gives us 3 visible peaks in an asymmetric environment. We see clearly here how implementing this ITO layer allows for sharp peaks in this environment. Starting from the highest-λ one, this one resembles a LSPR peak : wide, high-intensity, and unrelated to in-plane diffraction. The other 2 are, however, much thinner and linked to the Rayleigh anomalies of the 2 directions of the lattice.

These peaks stem from a collective resonance similar to SLR, linked both from Rayleigh Anomaly and the waveguided mode inside the ITO layer.

Unlike in standard SLR, waveguided SLR presents two peaks related to the Rayleigh anomalies of the 2 directions for the same polarization, although not at the same intensity. In SLR, only one peak is present for 1 polarization, since the interaction for the particles not in plane with the polarization doesn't affect the fields (see theory).

5.4 Comparison with simulations

Optical simulations of the structure were done in COMSOL by PhD student Hugo-Saint-Olive. They are finite element simulations using wave optics module. The sample is first modeled as a single particle fig. A.1. This structure is then repeated using Floquet's periodic conditions to create a 3D simulation of an infinite 2D lattice of nanoparticles.

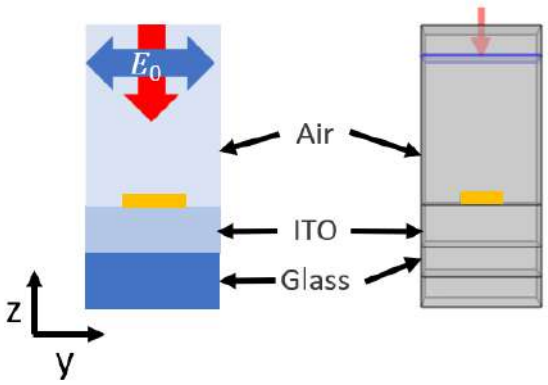


Figure 25: Left : Schematic of the cross-section of the sample along y. Incident wave vector and polarization are shown with the red and blue arrows. Right :Screenshot of the periodic COMSOL model structure. The red arrow correspond to where the incident field comes from. The bottom and top layers are PML (Perfectly Matched Layers), used to process infinite boundaries in calculation and on this zone resonance boundaries are set.

These results offer a basis to compare our experimental results. From the simulations, it is possible to extract the extinction spectra as well as the field distributions at resonance inside the sample.

Simulated extinction spectrum

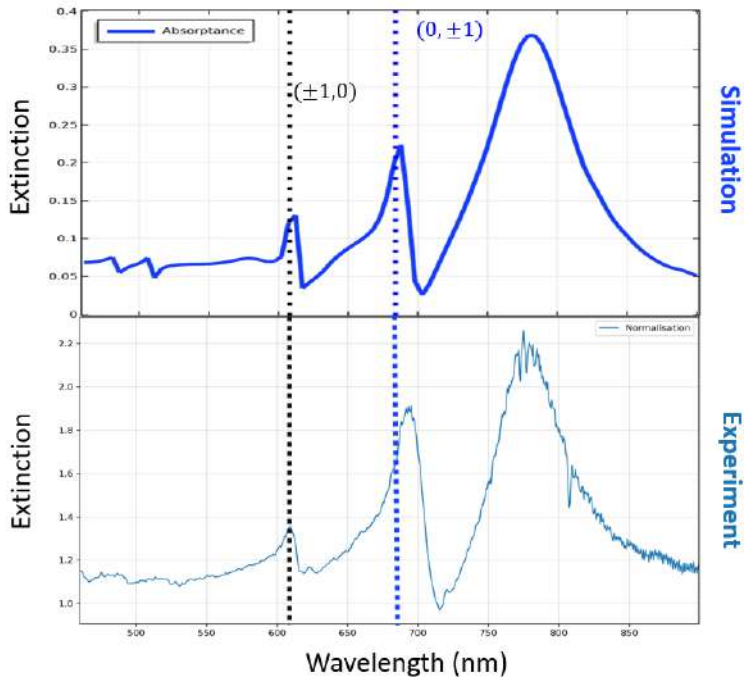


Figure 26: Top : Simulated absorption spectrum for a sample with glass/ITO sample. The periods are here of 400nm along x and 450nm along y. Incident light is polarized along y. Black and blue dashed lines represent the 1^{st} order Rayleigh anomaly condition along x (black) and y (blue) (for n_{eff}=1.52, taken as indicative). Bottom : Experimental extinction spectrum, the same as in fig. 24.

Looking at fig. 26, we see clearly how similar the experimental and simulated results are. Both the position and the shapes of the peaks are the same. This is a very good result that confirms the nature of the resonance peaks.

Field distributions inside the sample

To look further into the nature of our peaks, it is interesting to look at the fields distributions in the COMSOL model.

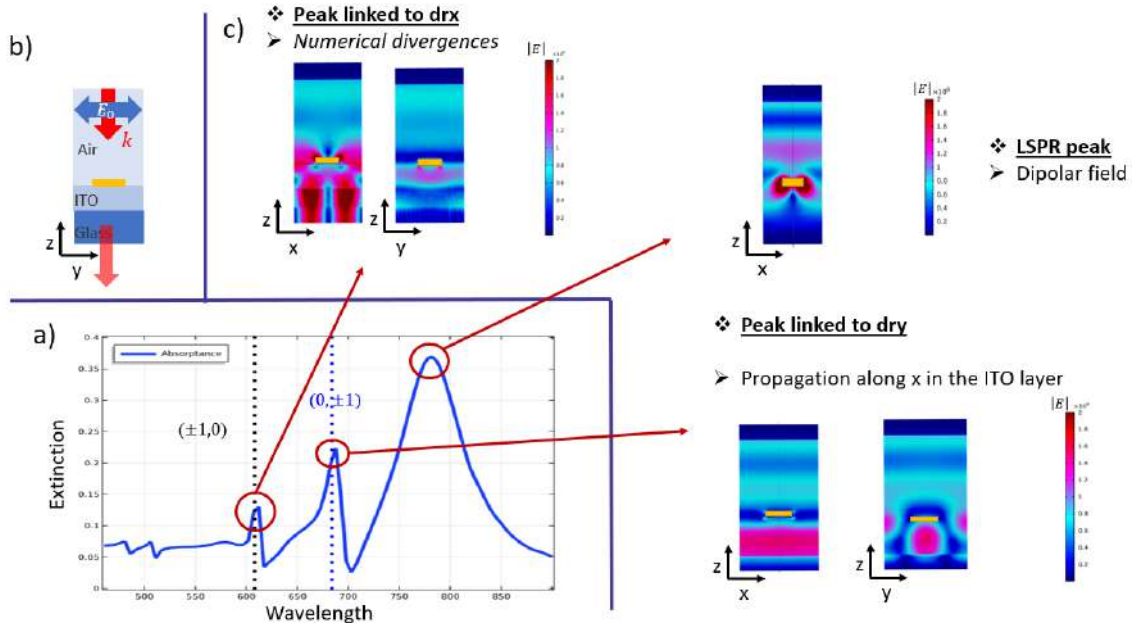


Figure 27: a) Simulated absorption spectra, same as in fig. 26. The polarization remains along y. b) Schematic representing the cut of the sample in the model. Incident light is represented, as well as all the different layers of the samples. c) Field distribution cuts along x and y of the simulated model of the samples, at the resonance peaks. The gold rectangle represents one single particle.

Looking at the highest wavelength peak, we see that the electric field is high around the single nanoparticle, exhibiting no collective mode. This is confirmed because when changing the period, this peak does not move. This strengthens the hypothesis of this peak being related to LSPR.

For the 2 sharp peaks which correspond to the Rayleigh anomalies linked to the 2 directions, the field distributions are slightly different. For the y direction, which is the also the polarization of the incident light, we have a strong field in the ITO region. This mode is propagating along the x direction, and couples all the particles together. For the x direction (perpendicular to the polarization of the incident light), the field distribution exhibit some numerical divergences.

Influence of the polarization

Changing the polarization of the incident light gives a different extinction spectrum :

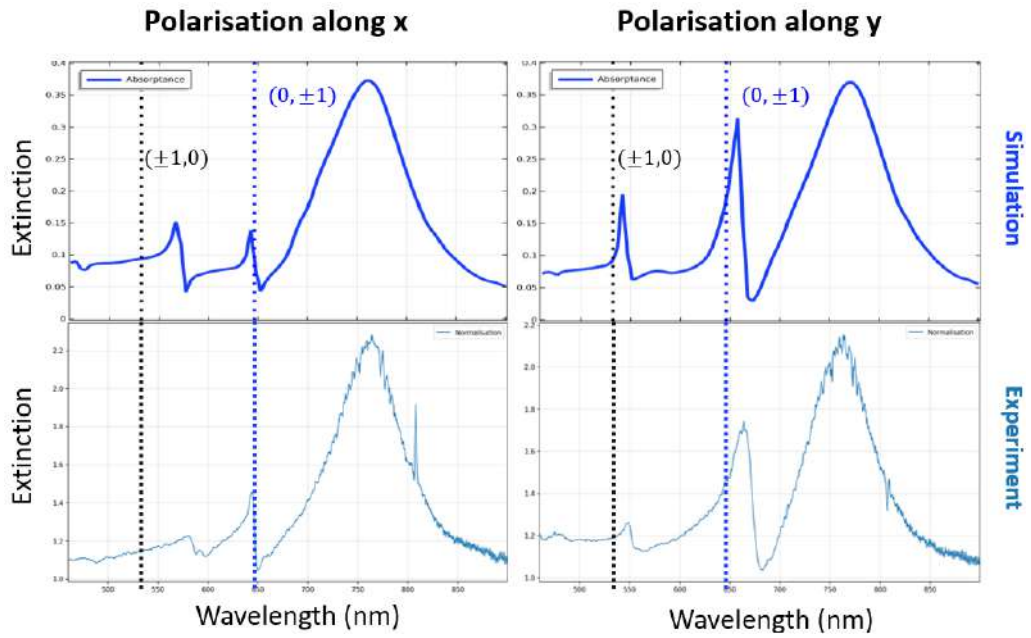


Figure 28: Left : Simulated and experimental extinction spectra for a sample of period 350nm along x and 425nm along y. The polarization of the incident light is along x. Right : Simulated/experimental spectra for the same sample, but with the polarization of the incident light along y.

We notice a significant shift in peak intensity, and a slight shift concerning the position of the peaks. However, there are still the same number of peaks, and their overall shape remains unchanged (2 sharp, 1 wide).

5.5 Conclusion and perspectives

Characterization of several samples of different periods allowed for 2 things :

-Confirmation of the concordance between the experimental and simulated spectra for different parameters

-Choice of a specific set of period picked because the quality of the peak as well as its position (close to where we will want to excite the QD).

One good set of samples is the one showcased in fig. 24. For the resonance at around 685nm, we found a Q of around 30 (calculated from the extinction spectrum fig. 24), which is higher than an LSPR Q (around 10). This exciting result allows to have a great baseline to go to the creation of the lattices.

6 Creation of cavities

Now that we managed to fabricate high-quality nanoparticle arrays that exhibit collective resonance, the next step is to create over these sample a cavity that would enable coupling with our nanoemitters, as described in [6].

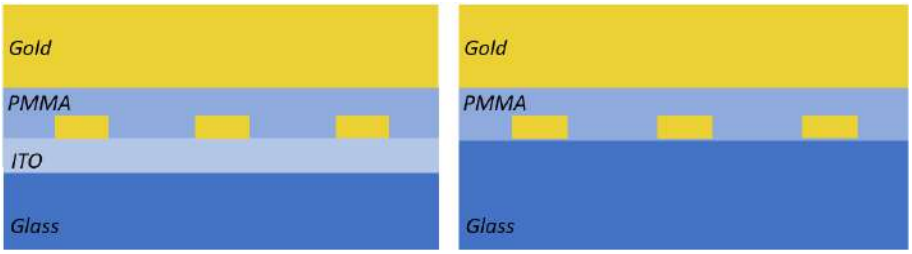


Figure 29: Schematic of samples which will enable a cavity. A layer of PMMA of thickness ranging from 20nm to 100nm and a thick layer of gold were deposited on top of the nanoparticle array, either with an ITO substrate in left, or a glass substrate in right.

The new structure of our samples is showcased in fig. 29, while a picture of one of them is shown in fig. 30. The ITO layer is usually around 140nm, while the thickness of PMMA layer is 20nm.

One important thing to notice about this structure is that the refractive index of the superstrate (when considering the particle array) has changed. The refractive index of PMMA being close to the one of glass, we are now in the case of a symmetric environment if we only have a glass substrate (no ITO, as pictured in fig. 29 right). This leaves the opportunity to fabricate samples without the ITO layer, which should exhibit standard SLR, as described in the theoretical part.

6.1 Cavity theory - Purcell effect

By definition, an optical cavity is an arrangement of opposing mirrors that let light reflect back and forth in it. By doing so, the cavity exhibits resonant modes, in which the electromagnetic field is very strong. In the case of fig. 29, it is gold that serves as mirror to create the cavity. This means that the cavity is located between the thick gold layer and the nanoparticle.

By implementing a quantum emitter inside this cavity, its emission can be either enhanced or suppressed. This phenomenon is called **Purcell Effect** [10], and is due to the modification of the density of optical states in the cavity compared to in free space. When the emitter's transition frequency matches a resonant mode of the cavity, its emission rate is multiplied by the Purcell factor, which is written as:

$$F_P = \frac{3}{4\pi^2}\left(\frac{\lambda}{n}\right)^3 \frac{Q}{V} \tag{10}$$

with $\frac{\lambda}{n}$ the wavelength inside the medium, Q the quality factor of the cavity and V the volume of the mode.

By increasing Q, or minimizing V, you can thus increase greatly the spontaneous emission of a quantum system (here a quantum dot).

6.2 Fabrication of the cavities

To create those cavities, we need to first have a sample with good-quality nanoparticle arrays. This sample is then cleaned the same way that in 3.2.2. A layer of 1% PMMA in anisole, which correspond to a 20nm thick layer after baking, is deposited by spin-coating and hard baking, with the same parameters as in 3.2.3.

Homogeneity of the layer has to be extremely good in order to have cavities of the same length all throughout the lattice. To do so, special care has to be taken when depositing the PMMA before spincoating.

The 100nm thick layer of gold, which serves as one mirror of the cavity, is deposited by PVD, in the same way as described in 3.2.5. The layer of titanium used beforehand to stick to the glass is not necessary anymore with PMMA, since gold sticks easily to this material.

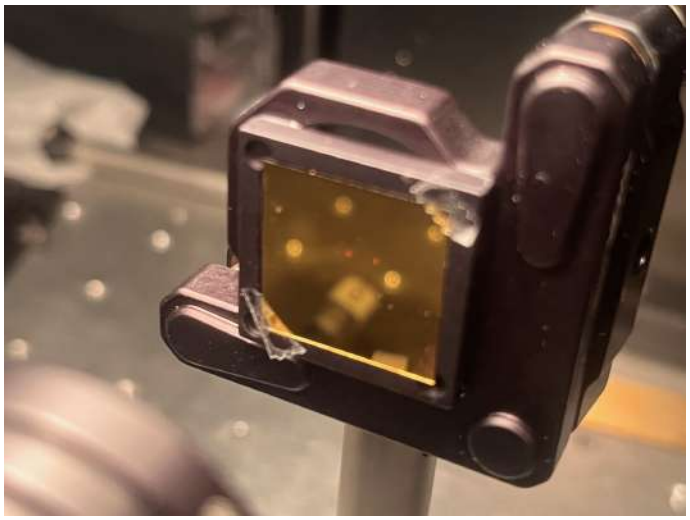


Figure 30: Picture of a sample which enables cavities. The tiny red dots here are the lattices, which diffract light.

6.3 Characterization

The deposition of the 100nm layer of gold makes it impossible to retrieve a relevant transmission spectrum such as before, since light does not cross the sample anymore. The experimental setup thus has to be re-imagined, this time in reflection.

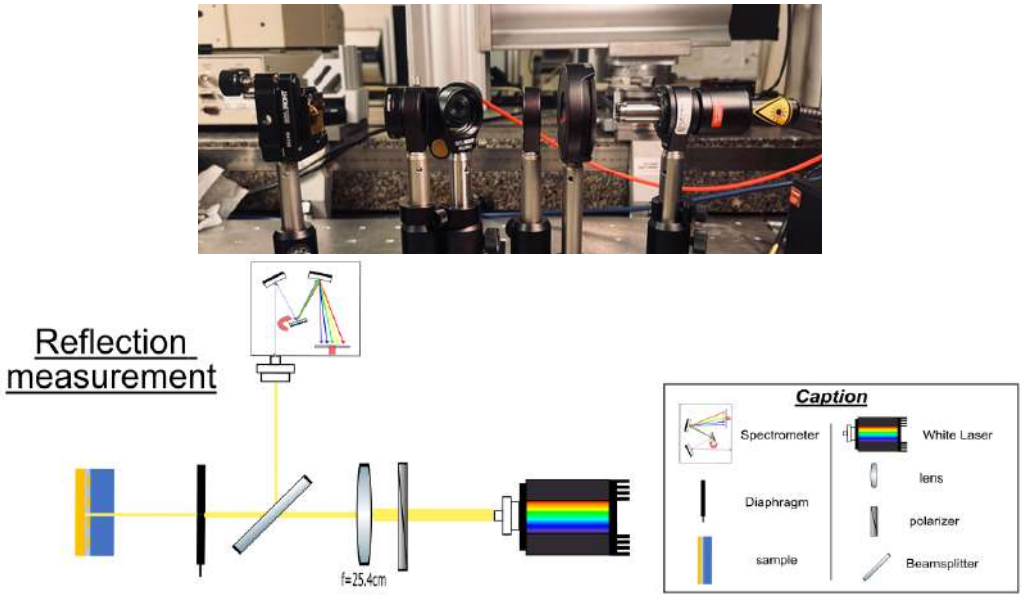


Figure 31: Top : Picture of the experimental setup in reflection in the laboratory. Bottom : Schematic of the experimental setup in reflection.

The light passes trough a polarizer and a lens which are the same as the setup in transmission. However, a beam splitter is implemented between the lens and the diaphragm. The beam first goes through the splitter and enters the sample by the glass substrate. It is reflected totally inside the sample by the thick gold patch at the top, and is sent by the beam splitter into a collimator. This collimator will lead the light to the spectrometer. Two reference spectra are still needed such as before (reference and lattice signals), but here it is difficult to find a proper reference signal, possibly because the gold reflection is not perfect. This problem, along with the fact that the reflection setup is harder to align optically, makes for slightly noisy extinction spectra. However, this setup is still being improved to have better results. The reference taken here is the beam reflected by the thick gold layer, but without passing through the lattice.

6.4 Cavity extinction spectra : sample with ITO substrate

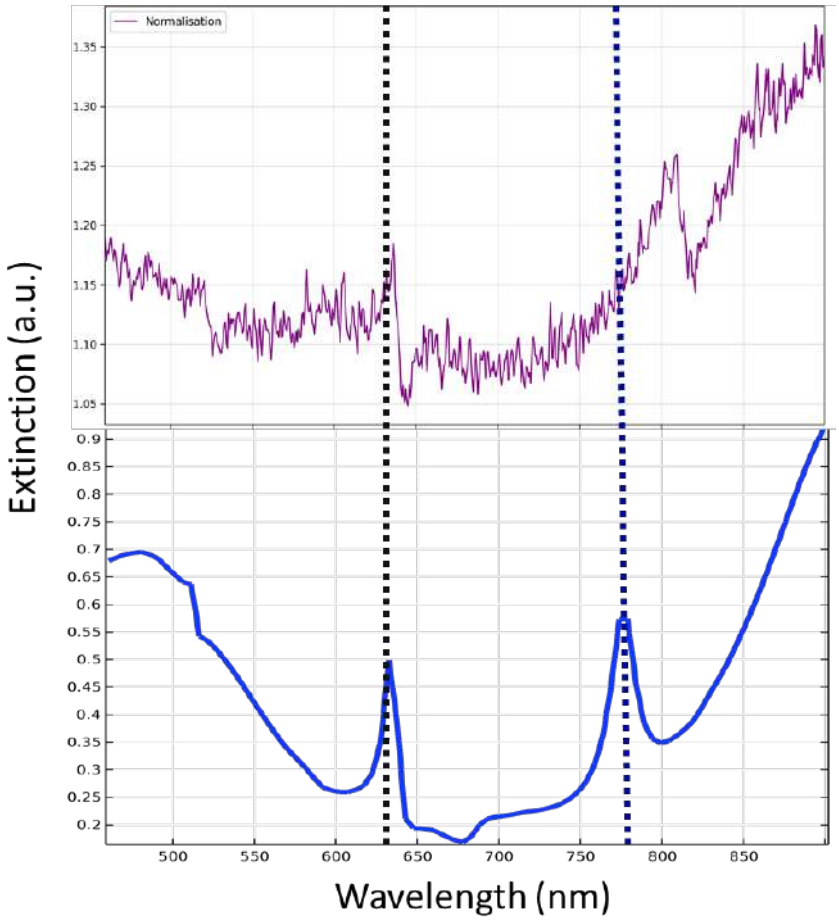


Figure 32: Top : Experimental extinction spectrum of a sample with an ITO substrate and of period 450nm along x, 400nm along y. The polarization of the incident field is along y. Bottom : Simulated extinction spectrum of the same sample (same periods and polarization). Dotted vertical lines are at the top of each peak.

In fig. 32, we can see that there are peaks occurring at the same wavelengths as in simulation, especially at 640nm. This ultimately means that the collective resonance still happens with those new samples, even with the new layers. This is very promising, as it means that the coupling between these peaks and the nanoemitters is still possible.

6.5 Cavity extinction spectra : sample without ITO substrate

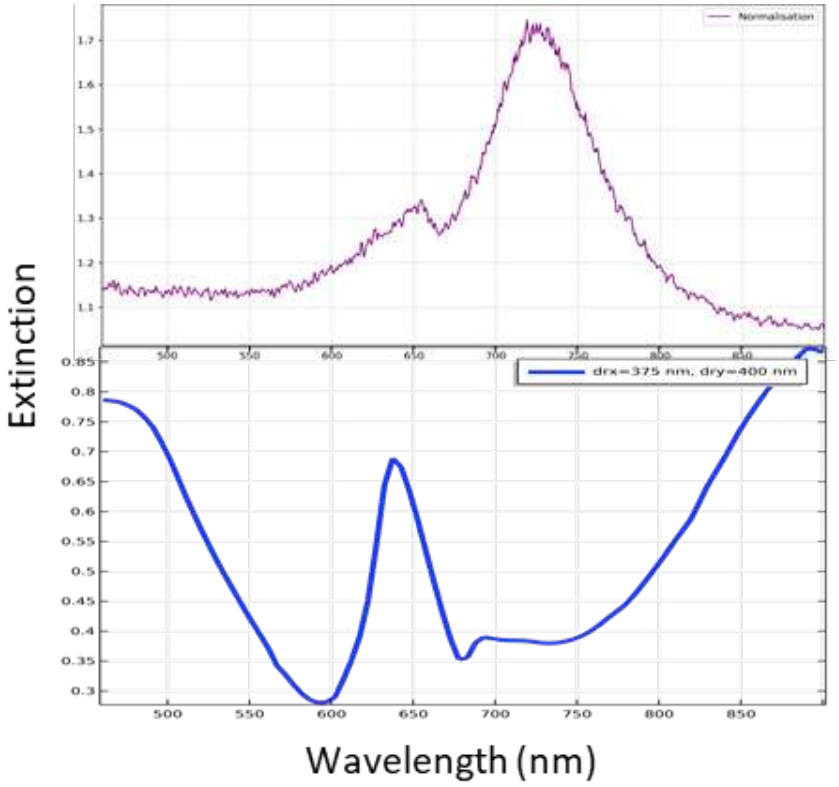


Figure 33: Top : Experimental extinction spectrum of a sample with an ITO substrate and of period 375nm along x, 400nm along y. The polarization of the incident field is along y. Bottom : Simulated extinction spectrum of the same sample (same periods and polarization).

Without an ITO substrate, the simulation expects the sample to have one sharp SLR peak at around 650nm. Experimentally, we obtain a result which is slightly different. The LSPR peak is still present, while a very small peak around 650nm remains present. This discordance between simulation and experimentation means that there is something missing in the simulation to properly understand what is happening in experimentation. Theoretically the peak is not very thin, which means that either the system is not really symmetric or the effective index of the PMMA is very different to the glass index.

7 Introducing nanoemitters on top of the lattice

7.1 Quantum Dot introduction

Quantum dots (QDs) are semiconductor particles a few nanometres in size with optical and electronic properties that differ from those of larger particles via quantum mechanical effects [12]. They are a central topic in nanotechnology and materials science. When a quantum dot is illuminated by UV light, an electron in the quantum dot can be excited to a state of higher energy. In the case of a semiconducting quantum dot, this process corresponds to the transition of an electron from the valence band to the conduction band. The excited electron can be relaxed into the valence band releasing its energy as light. The wavelength of that emission depends on the energy difference between the discrete energy levels of the quantum dot in the conduction band and the valence band.

7.2 Presentation of the QDs used

The quantum dots we will use further on are synthetized by PhD student Fengzhi Gu at Laboratoire de Physique et d'Etude des Materiaux (LPEM/ESPCI). They are 2-level Quantum Dots, with a CdSe core and a CdS shell. The diameter of the core is usually around $3nm$, while the total diameter of the dot is at $20.2 \pm 2nm$.

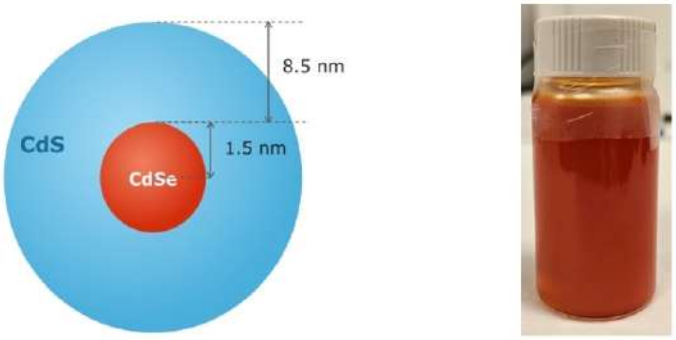


Figure 34: Left : Schematic of a CdS/CdSe Quantum Dot. Right: Picture of the solution containing quantum dots.

In fig. 34, the emission of the solution is in the visible, more particularly in the red. This emission changes when we go from the quantum dot solution to the single quantum dot. The absorption and emission spectra for a single quantum dot are shown in fig. 35.

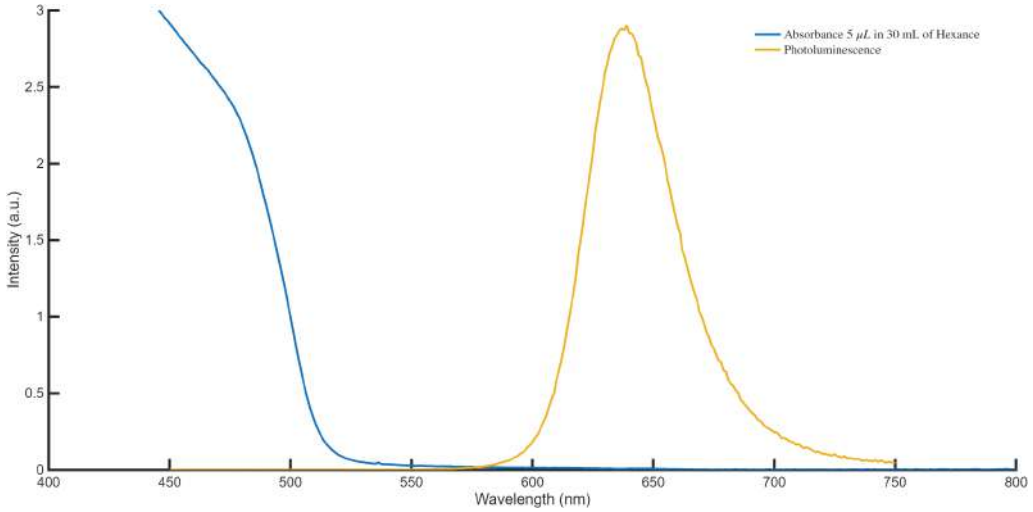


Figure 35: Schematic representing the photoluminescence (in yellow) and absorption (blue) of a single Cd/CdSe quantum dot. The absorbance is found with a concentration of 5 µL of QD in 30mL of hexane.

As seen in fig. 35, the CdS/CdSe quantum dots absorb light in the UV, and reemit light in the visible range, at around 640 nm.

7.3 Deposition of nanoemitters on a sample

To deposit those quantum dots onto a sample, we first need to dilute the solution (the one in fig. 34 right), in order to have quantum dots which are deposited individually.

The solution is diluted in hexane, creating solutions with concentrations in the range of 10^{-4} to 10^{-6}, which will be deposited on a glass substrate to determine the right concentration.

Spin-coating of the Quantum Dots : Depositing QDs is much harder than depositing PMMA because hexane has very low viscosity and evaporates fast. The emitters must be then be spincoated very quickly and at high speed. 50 µL of the QD solution is deposited on the sample before spincoating. The parameters used are 10 seconds at 3000 rpm.

The sample is then observed under UV light in a microscope, with the sample being upside down.

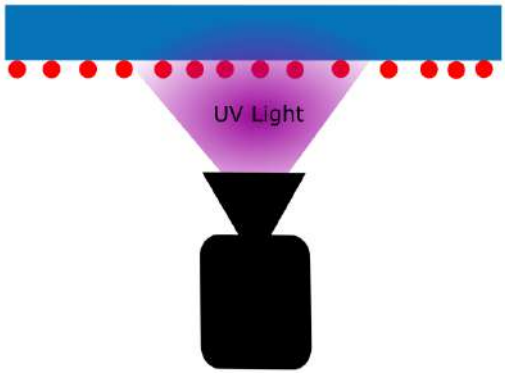


Figure 36: Schematic of the observation, on an Olympus microscope IX71 of the Quantum Dots on a glass substrate.

To observe the isolated quantum dots emission, the sample need to be observed under an X100 objective.

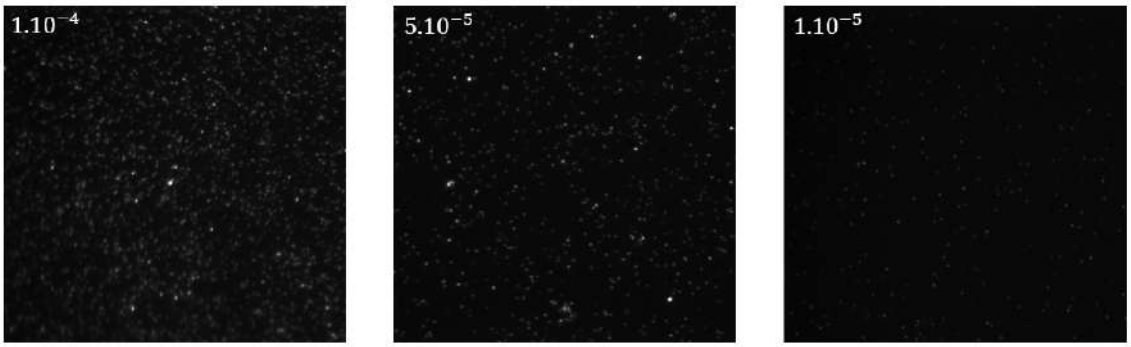


Figure 37: Pictures, under UV light and with an objective x100, of 3 different samples covered with 3 different concentrations of QD solutions.

In fig. 37, we see that the small dots are all the quantum dots. For a concentration of 10^{-4} and 5.10^{-5}, there are a lot of quantum dots on the sample, which create amalgamations. Since we want isolated emission, having QDs that close to each other is not what is wanted. For a concentration of 1.10^{-5}, there are still a good quantity of quantum dots, but without being too close to one another (distance between 2 QD needs ideally to be around 2 to 3µm. This is this concentration that will be kept later on for the characterization.

7.4 Characterization of the Quantum Dots in the lattice

A solution of this specific concentration of Quantum Dots was thus deposited on the samples with nanoparticle lattices.

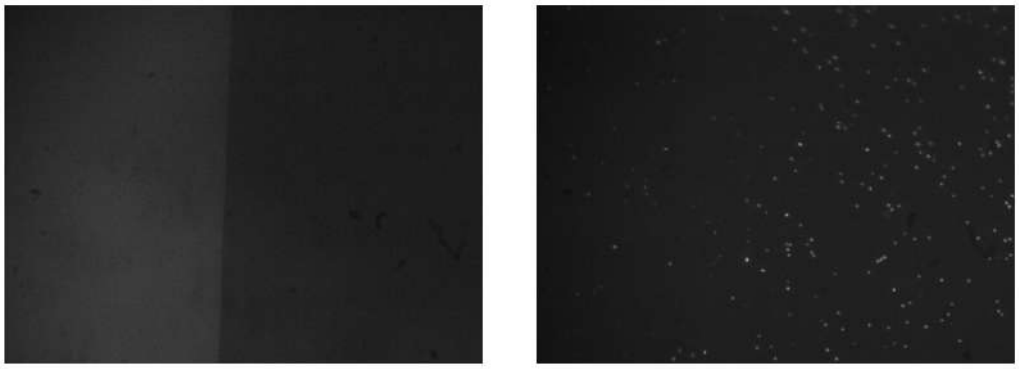


Figure 38: Left : Picture of the extremity of one nanoparticle array in my sample. It was taken using a X100 objective coupled with an Olympus IX71 microscope and a camera coupled with the software *Infinity analyze*. Right : Picture of the extremity of the array with the same parameters but this time under UV light.

I did the characterization of single quantum dots emission using a custom optical setup shown below.

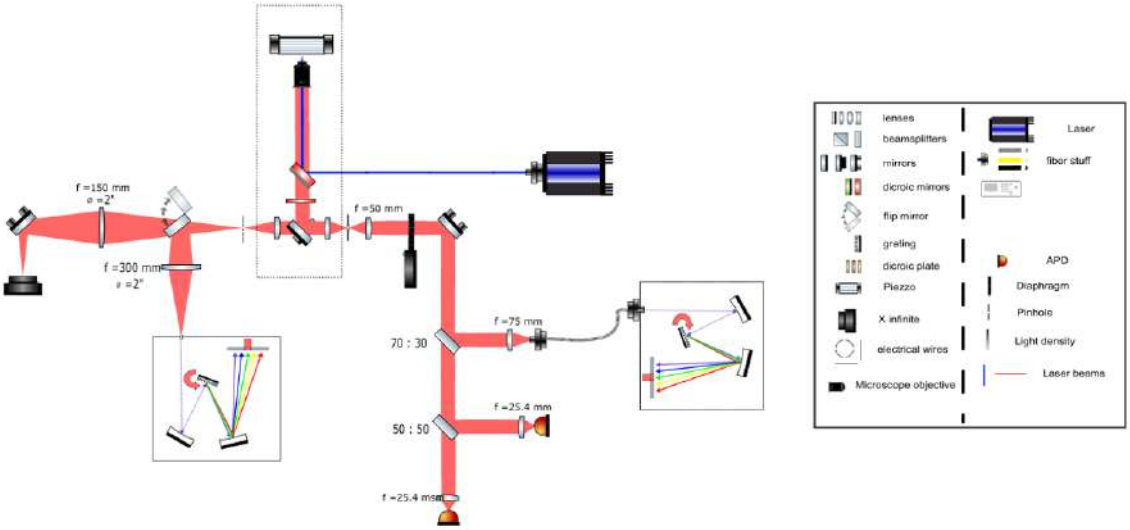


Figure 39: Schematic of the optical setup used here for optical characterization, spectrometry and lifetime of nanoemitters.

The sample is first looked at under visible light to do the focus. Afterwards, a pulsed laser is impinged onto the sample, focused on the part of the sample the lattice is. With a camera, we aim the laser next to a QD in the sample. A piezoelectric motor scans a small range of the sample with the laser. The emitted light by the sample is gathered by an avalanche photodiode (as shown in fig. 39). Once the scan is over, we obtain a map of the intensity of the emitted light in the scanned zone. If a Quantum Dot is present in this zone, it will appear as a bright spot.

To retrieve the emission spectrum of one single quantum dot, we use a pinhole which allow to aim exactly at a spot in the sample, by clicking on a part in the scanned

zone. Once this is calibrated, we can extract various relevant pieces of information, like correlation of light (using Hanbury-Brown-Twiss setup already implemented onto the setup), lifetime characterization and more.

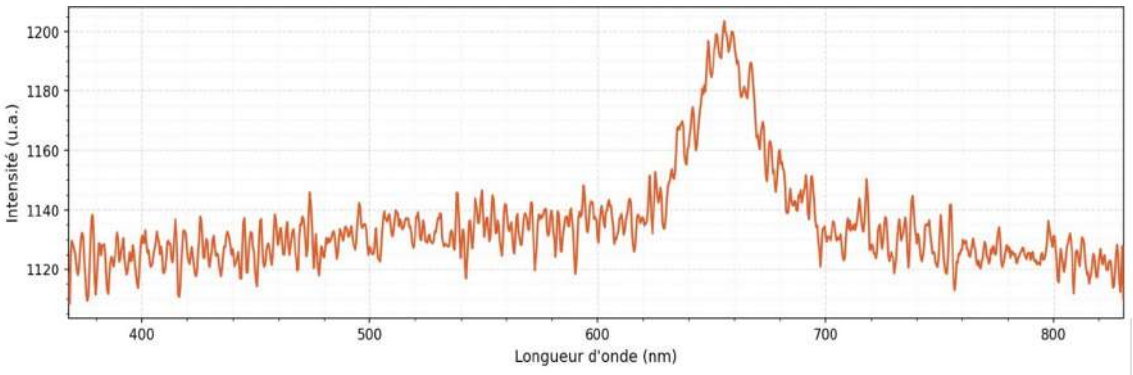


Figure 40: Emission spectrum of a single quantum dot on a lattice. Exposition time is 10 sec, repetition rate of the pulsed laser is 0.5 MHz.

This spectrum present an emission peak at 660nm, which is the same as in fig. 35, confirming that what we see now is the emission of the quantum dot.

8 Introducing nanoemitters inside the cavities

8.1 Preliminary study - Optimal PMMA thickness for QDs

Context

One critical aspect of the creation of cavities with Quantum Dots inside of them is the ability of keeping the emission of the emitters alive while creating them. This problem is possibly due to the modification of the electronic composition of the QDs, when in contact to gold at 1000°C during PVD. Similar study has already been done by previous PhD candidate Amit Dhawan [5], but since we are now using different nanoemitters, this experiment needs to be done again.

The thickness of this layer needs to be optimized in order to have both big enough thickness to protect the emission of the QDs, while having a small enough thickness to exhibit good coupling conditions (see coupling theory).

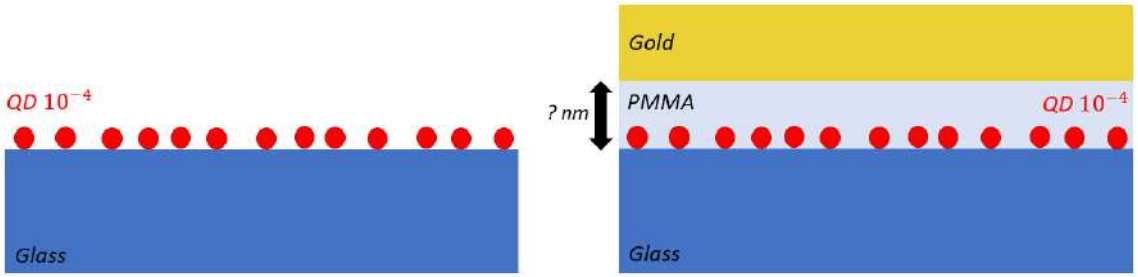


Figure 41: Left : Schematic of the sample consisting of a glass substrate and a deposited QD solution of 10-4 of concentration. Right : Schematic showing this same sample with an added PMMA layer, whose thickness will be varied to be optimized, and a 100nm thick layer of gold.

Experiment

The process of the experiment is as follows :

Quantum Dot deposition : 50µL of a solution of concentration 10^{-4} is deposited using a pipette on a glass substrate, and spread out homogeneously with a spincoater (just like before).

PMMA deposition : The concentration of PMMA deposited on top of the QDs is varied depending on the samples : from 0 nm (no PMMA) to 200nm thickness of the layer.

PMMA is deposited via spin-coating and hard bake with the usual parameters.

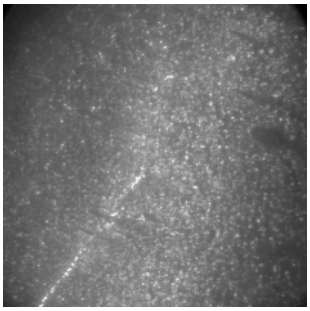
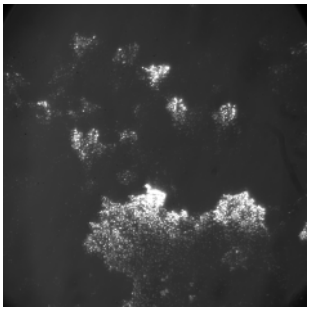
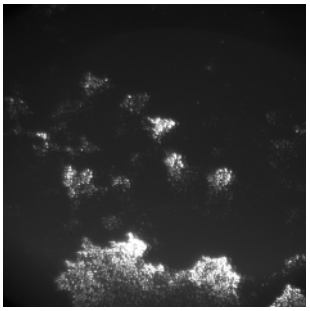
Gold deposition : 100nm Gold layer is deposited on top of the sample using PVD. This step is critical, since it can kill the emission of our emitters, because of the harsh conditions of deposition. The layer of PMMA will act as a layer of protection during this step.

Table 2: PMMA thickness according to the massic concentration of PMMA

Concentration (%)	**Thickness (nm)**
0.5	$\approx 10nm$
0.9	$\approx 20nm$
1.5	$\approx 35nm$
2	$\approx 50nm$
3	$\approx 100nm$

Pictures before and after deposition were done to have a proper comparison, for all the different PMMA thicknesses.

Table 3: Images before and after Au deposition, depending on PMMA thickness. Exposition rate = 2500ms.

PMMA layer thickness (nm)		
10		
20		

As seen clearly in table 3, a PMMA layer of 10nm is not enough to protect QD emission during the gold deposition process. However, a 20 nm layer allows to keep the QD emission untouched. This thickness is optimal, as it allows also to have a thin cavity for coupling.

8.2 Perspectives

Once the thickness of the PMMA layer has been set to 20nm, we can fabricate samples with quantum dots in between the layers. This gives us the baseline to start characterization of the quantum dots emission coupled with plasmonic cavities, which is the next big step.

9 Conclusion

In this work, the manipulation of light-matter interactions at the nanoscale was successfully advanced through the implementation of collective patch antennas powered by Plasmonic Surface Lattice Resonance (SLR). The primary objective of transitioning from single patch antennas to collective lattice structures to enhance the emission of nanoemitters was tackled through nanofabrication, optical characterization, and numerical simulations.

I first mastered the fabrication of high-quality gold nanoparticule arrays exhibiting SLR, using and optimizing a 5-step process flow in order to have the best sample possible. These samples were characterized by a transmission optical setup, where sharp, high-Q resonance peaks were shown when using an ITO substrate in an asymmetric environment.

Experimental extinction spectra have excellent concordance with the spectra modeled with the COMSOL software. This agreement successfully validated the physical nature of the waveguided resonance modes propagating through the ITO layer.

Samples with gold cavities were fabricated and characterized using a reflection setup, showing promising results : The SLR peaks were still visible in experimentation.

Finally, quantum dots were studied on the nanoparticle lattice to study their emission. Preliminary studies were also done to prepare for the implementation of those nanoemitters inside the cavities.

With the baseline fabrication and coupling parameters firmly established, the next step is to study single nanoemitters embedded directly inside the plasmonic cavities. Future work will focus on performing lifetime characterization and photon correlation measurements to quantify the exact spontaneous emission enhancement driven by the Purcell effect. Ultimately, these collective patch antenna architectures provide a promising way of developing efficient and coherent single-photon sources for quantum technologies and photonics.

Acknowledgments : I would like to thank the NANOOQ team I worked with at INSP, and especially my 2 supervisors *Agnès MAITRE and Hugo SAINT-OLIVE* for their guidance and support during this internship. I would also like to thank *Erwan Dandeu* for his trainings in the clean-room, *Fengzhi Gu* and *Juliette Lignères* for their expertise in Quantum Dots characterization as well as all the interns and PhD students I met at INSP during this period that made this internship a really pleasant stay.

Bibliography

[1] Baptiste Auguié et al. "Diffractive arrays of gold nanoparticles near an interface: critical role of the substrate". In: *Physical Review B* 82.15 (Oct. 27, 2010), p. 155447. ISSN: 1098-0121, 1550-235X. DOI: 10.1103/PhysRevB.82.155447. arXiv: 1007.4428[physics.optics]. URL: http://arxiv.org/abs/1007.4428 (visited on 06/10/2026).

[2] C. Belacel et al. "Controlling Spontaneous Emission with Plasmonic Optical Patch Antennas". In: *Nano Letters* 13.4 (2013), pp. 1516–1521. DOI: 10.1063/nl3046602.

[3] Y. Chu et al. "Experimental Observation of Narrow Surface Plasmon Resonances in Gold Nanoparticle Arrays". In: *Applied Physics Letters* 93.18 (2008), p. 181108. DOI: 10.1063/1.3012365.

[4] M. Dewynter et al. "Broadening the Plasmonic Spectral Range of Metallic Metasurfaces Using Dual-Material Arrays". In: *Nano Letters* 26.6 (Feb. 2026), pp. 2223–2228. ISSN: 1530-6984, 1530-6992. DOI: 10.1021/acs.nanolett.5c05943. URL: https://pubs.acs.org/doi/10.1021/acs.nanolett.5c05943 (visited on 06/10/2026).

[5] Amit Raj Dhawan. "Deterministic lithographic fabrication of single emitter plasmonic patch nanoantennas, and their characterization". 2016PA066753. PhD thesis. 2016. URL: https://theses.fr/2016PA066753/document.

[6] James T. Hugall, Anshuman Singh, and Niek F. van Hulst. "Plasmonic Cavity Coupling". In: *ACS Photonics* 5.1 (2018), pp. 43–53. DOI: 10.1021/acsphotonics.7b01139.

[7] Alastair D. Humphrey and William L. Barnes. "Plasmonic surface lattice resonances on arrays of different lattice symmetry". In: *Physical Review B* 90.7 (Aug. 7, 2014), p. 075404. ISSN: 1098-0121, 1550-235X. DOI: 10.1103/PhysRevB.90.075404. URL: https://link.aps.org/doi/10.1103/PhysRevB.90.075404 (visited on 06/10/2026).

[8] V. G. Kravets et al. "Plasmonic Surface Lattice Resonances: A Review of Properties and Applications". In: *Chemical Reviews* 118.12 (June 27, 2018), pp. 5912–5951. ISSN: 0009-2665, 1520-6890. DOI: 10.1021/acs.chemrev.8b00243. URL: https://pubs.acs.org/doi/10.1021/acs.chemrev.8b00243 (visited on 06/10/2026).

[9] Matthew Pelton, S. David Storm, and Haixu Leng. "Strong coupling of emitters to single plasmonic nanoparticles: exciton-induced transparency and Rabi splitting". In: *Nanoscale* 11 (31 2019), pp. 14540–14552. DOI: 10.1039/C9NR05044B. URL: http://dx.doi.org/10.1039/C9NR05044B.

[10] Edward Mills Purcell. "Spontaneous emission probabilities at radio frequencies". In: *Physical Review* 69.11-12 (1946), p. 681.

[11] Håvard S. Ugulen et al. "Experimental and theoretical investigation of waveguided plasmonic surface lattice resonances". In: *Optics Express* 30.21 (Oct. 10, 2022), p. 37846. ISSN: 1094-4087. DOI: 10.1364/OE.470017. URL: https://opg.optica.org/abstract.cfm?URI=oe-30-21-37846 (visited on 06/10/2026).

[12] Wikipedia contributors. *Quantum dot — Wikipedia, The Free Encyclopedia*. [Online; accessed 2-July-2026]. 2026. URL: https://en.wikipedia.org/wiki/Quantum_dot.

Appendix A

Gantt Diagram

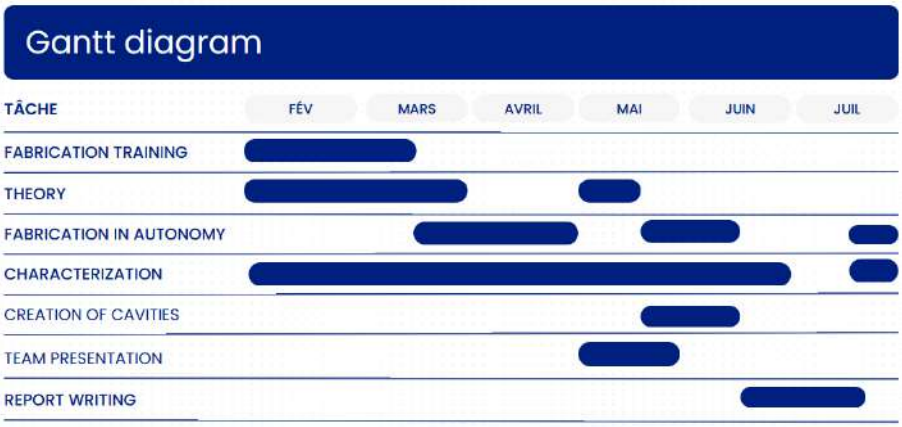


Figure A.1: Gantt diagram of the internship

Appendix B

Résumés

UK : During my internship at INSP, I had the opportunity to work on Plasmonic Surface Lattice Resonance (SLR), in the context of light-matter interaction in nanostructures. I first mastered the fabrication of high-quality gold nanoparticule arrays exhibiting SLR, using and optimizing a 5-step process flow in order to have the best sample possible. I characterized these samples by a transmission optical setup, where sharp, high-Q resonance peaks were shown when using an ITO substrate in an asymmetric environment, with great concordance between simulation and experimentation. This great result would allow to create samples with gold plasmonic cavities, which were fabricated and characterized using a reflection setup. We found promising results : The SLR peaks were still visible in experimentation. Finally, quantum dots were studied on the nanoparticle lattice to study their emission. Preliminary studies were also done to prepare for the implementation of those nanoemitters inside the cavities. This leaves room to further studies on the emission enhancement (or not) of the nanoemitter, when coupled to a plasmonic antenna with SLR.

FR : Au cours de mon stage à l'INSP, j'ai eu l'occasion de travailler sur la résonance plasmonique de réseau de surface (SLR), dans le cadre des interactions lumière-matière au sein des nanostructures. J'ai tout d'abord maîtrisé la fabrication de réseaux de nanoparticules d'or de haute qualité présentant une SLR, en utilisant et en optimisant un processus en cinq étapes afin d'obtenir le meilleur échantillon possible. J'ai caractérisé ces échantillons à l'aide d'un dispositif optique en transmission, qui a révélé des pics de résonance nets et à haut Q lors de l'utilisation d'un substrat ITO dans un environnement asymétrique, avec une excellente concordance entre la simulation et l'expérimentation. Ce résultat remarquable a permis de créer des échantillons dotés de cavités plasmoniques en or, qui ont été fabriqués et caractérisés à l'aide d'un dispositif en réflexion. Nous avons obtenu des résultats prometteurs : les pics de SLR étaient toujours visibles lors des expériences. Enfin, des points quantiques ont été étudiés sur le réseau de nanoparticules afin d'analyser leur émission. Des études préliminaires ont également été menées en vue de la mise en œuvre de ces nanoémetteurs à l'intérieur des cavités. Cela ouvre la voie à de nouvelles études sur l'amplification (ou non) de l'émission du nanoémetteur lorsqu'il est

couplé à une antenne plasmonique à SLR.

Louis AGARD

MNIS / Nanotech
2026

Institut des NanoSciences de Paris
4 place Jussieu, 75005 Paris

Surface lattice resonance in an array of gold nanoparticles

from 16/02/26 to 31/07/26

Under the supervision of :

- **Company supervisor : Agnès MAITRE, agnes.maitre@insp.upmc.fr**
- **Phelma Tutor : Liliana PREJBEANU, liliana.buda@cea.fr**

Resumé : Under electromagnetic excitation, metal nano-objects can support collective electron
oscillations, known as plasmon waves. For metal nanoparticles, this electrons oscillation
under the action of polarized optical wave excitation allows the nanoparticle to be assimilated to an oscillating dipole that absorbs and scatters light. When illuminated with
white light, a resonance (Localised Surface Plasmon Resonance, LSPR) can be observed

spectrally which the center and width, typically a few tens of nanometres, depend on the
dielectric constant of the metal and the shape of the nanoparticle. The spectral position of
the resonance is also very sensitive to the dielectric environment of the nanoparticle. This
property makes it possible to create sensitive sensors based on the detection of LSPR resonance shifts when the nanoparticle's environment changes. However, the sensitivity of
these sensors is limited by the width of the LSPR resonance. To increase sensitivity, these
nanoparticles can be positioned as a lattice on a substrate. Given the periodicity of this arrangement, the first order diffraction of incident light at a given wavelength can propagate in the plane of the array. This results in a resonance that is much thinner spectrally than that of LSPR and can be used to increase the sensitivity of the sensor. This
resonance is called Surface Lattice Resonance (SLR).
As part of this internship, we will use electron beam lithography to create arrays of gold nanoparticles on a substrate, enabling us to observe lattice resonances (SLR). We will characterize them optically and optimize the parameters to maximize the signal and its spectral finesse. In a second step, we will deposit CdSe/CdS quantum dots that resonate or
do not resonate with the SLR modes, and study how their emission is modified by the resonance.

Moyens : One team of 5 persons (3 PhD, 1 engineer, 1 profesor), cleanroom facility (SEM, PVD,…) with one cleanroom engineer. 2 experimental room with laser, APDs,… . 1 computer, 2 monitors, stationary,…